PCR
TRICUSPID
Focus Group

Echocardiographic guide on tricuspid valve interventions

For more information about the PCR Tricuspid Focus Group

#PCRtricuspid

Supported by:

GE HealthCare

Project directors:

Dr. Julia Grapsa
Cardiologist / Imager
Guys and St Thomas NHS Trust – London, UK

Prof. Erwan Donal
Cardiologist / Imager
University Hospital of Rennes, University of Rennes – Rennes, France

Authors:

Dr. Yoan Lavie Badie
Cardiologist / Imager
Toulouse University Hospital – Toulouse, France

Dr. Aditya Bhalla
Cardiology fellow
Guys and St Thomas NHS Trust – London, UK

Prof. Augustin Coisne
Cardiologist / Imager
Lille University Hospital – Lille, France

Dr. François Deharo
Cardiologist / Imager
Marseille University Hospital (APHM) – Marseille, France

Dr. Nina Ajmone Marsan
Cardiologist / Imager
Leiden University Medical Center (LUMC) – Leiden, Netherlands

Dr. Denisa Muraru
Cardiologist / Imager
Istituto Scientifico Ospedale San Luca (Istituto Auxologico Italiano) – Milan, Italy

Dr. Laura Sanchis
Cardiologist / Imager
Clinical and Provincial Hospital of Barcelona – Barcelona, Spain

Dr. Marta Sitges
Cardiologist / Imager
Clinical and Provincial Hospital of Barcelona – Barcelona, Spain

Dr. Michele Tomaselli
Cardiologist / Imager
Istituto Auxologico Italiano – Milan, Italy

Dr. Edoardo Zancanaro
Cardiac Surgery Resident and Interventional Cardiology Fellow
IRCCS Ospedale San Raffaele – Milan, Italy

Senior reviewers:

Prof. Victoria Delgado
Cardiologist / Imager
Hospital Germans Trias i Pujol – Badalona, Spain

Prof. Luigi Badano
Cardiologist / Imager
Istituto Scientifico Ospedale San Luca (Istituto Auxologico Italiano) – Milan, Italy

Table of contents

TOE views – preprocedural – RV assessment

1. Midesophageal four-chamber view	• Overall RV anatomy and global function
2. Midesophageal RV inflow-outflow view	• Wrap-around view • Useful to assess RV free wall
3. Transgastric mid short-axis view	• Assessment of the RV free wall and ventricular septum
4. Transgastric RV inflow view	• Long-axis view of the RV
5. Midesophageal long-axis view	• Pulmonic valve can be seen anterior to the aortic valve • Portion of RVOT can be visualised
6. Transgastric RV outflow view	• Provides an image with many of the same structures seen in the midesophageal RV inflow-outflow view, including the RA, RV, PA
7. Deep transgastric RV apical view	• Focused RV, tricuspid valve, and RA

Table 1: Important TOE views for RV assessment

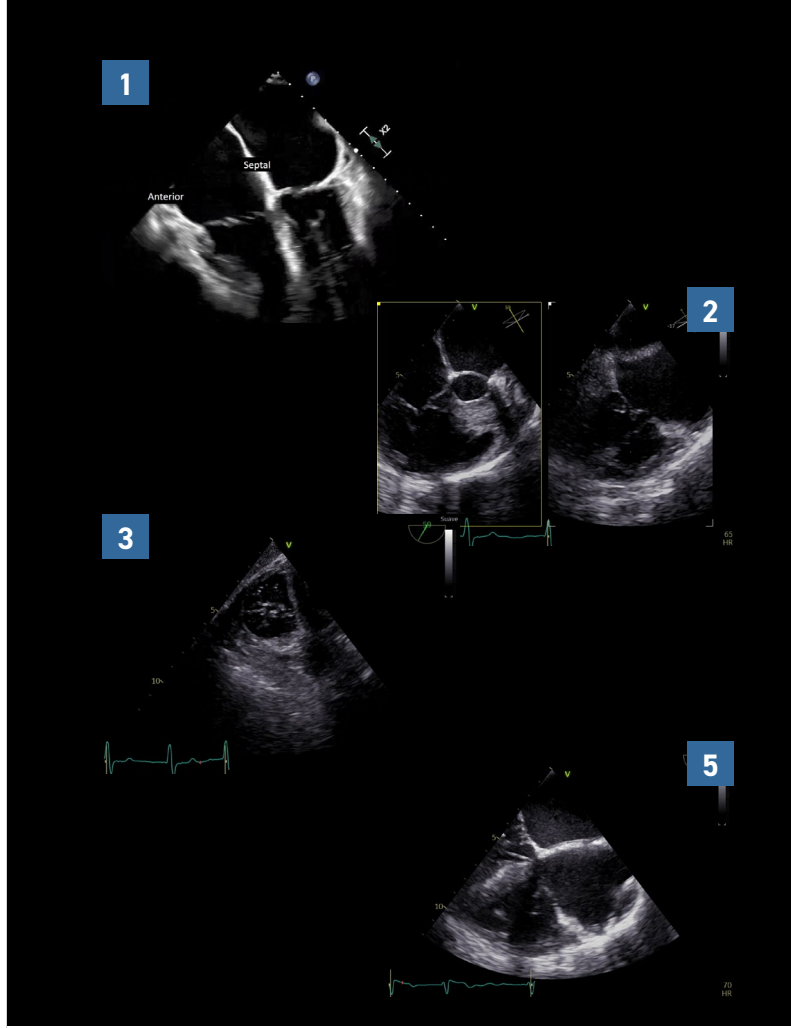

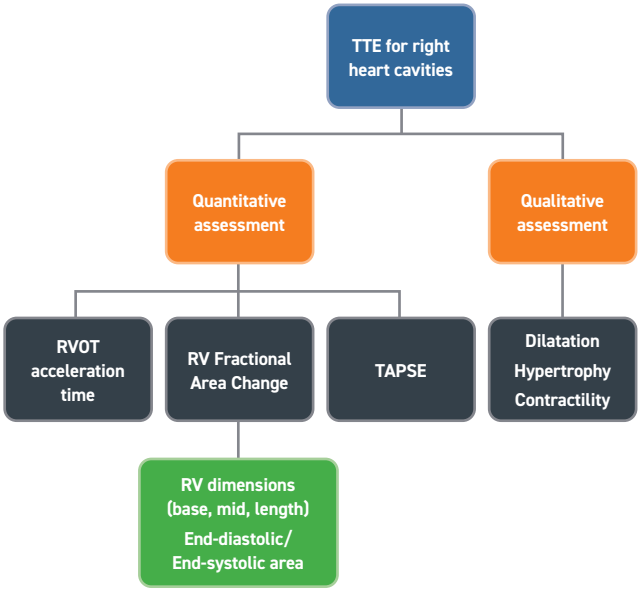

Supplement Figure 1: Initial assessment of right heart with transthoracic echocardiography: qualitative and quantitative approach
Abbreviations: TTE: transthoracic echocardiography, RVOT: right ventricular outflow tract, RV: right ventricle, TAPSE: tricuspid annular plane systolic excursion

Right heart chambers – preprocedural assessment

During preprocedural right heart assessment, it is important to assess the right ventricle (RV) qualitatively and quantitatively.

Transthoracic echocardiography (TTE):

Starting from TTE, the RV is being assessed from the following fundamental views:

1. Parasternal long axis view (RV inflow)
2. RV short axis view at the level of left ventricular (LV) papillary muscles (RV body)
3. RV short axis view at the level of the great vessels (RV outflow view)
4. Apical four-chamber view – RV-focused view
5. Subcostal view

The first step is to assess the RV in terms of size, systolic function, and hypertrophy. The RV is one-third the size of the left ventricle (LV) and has one-sixth of its mass. Important anatomical and physiological RV features should be taken into consideration during its assessment.[1] It is the most anterior chamber of the heart, with complex anatomy including the moderator band and the normal pressure within RV is less than 25 mmHg.

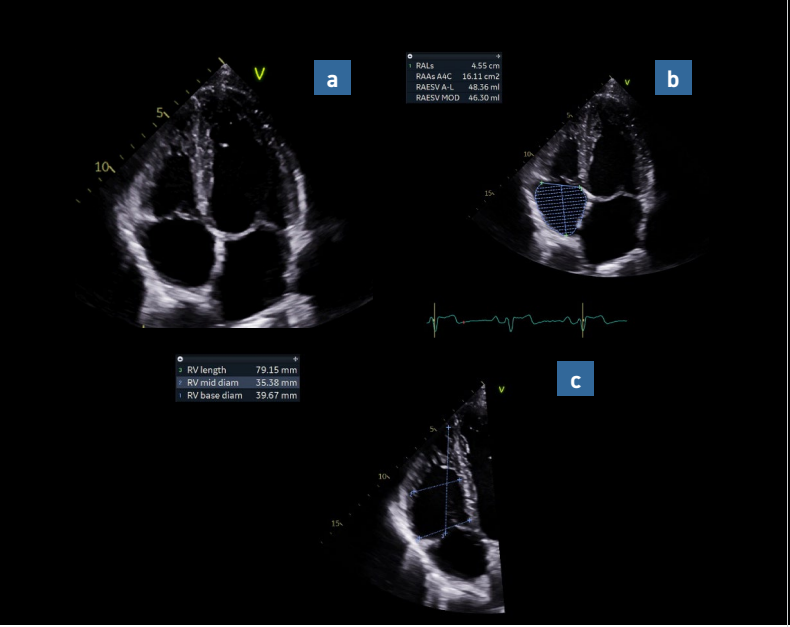

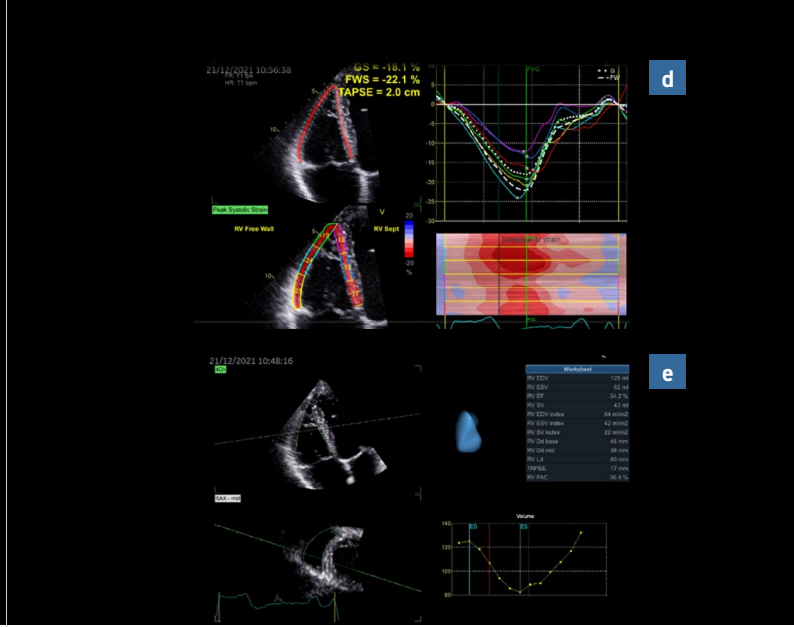

Figure 1: Right ventricular assessment (a) normal size of RV is 1/3 of LV (b) right atrial volumetric assessment with Simpsons (c) RV fractional area change (d) RV strain assessment (e) 3-dimensional assessment of volumes and ejection fraction
Abbreviations: *RV: right ventricle*

RV quantitative assessment

The full protocol for RV assessment essentially needs to include the following parameters:

1. RV outflow tract acceleration time (RVOT AT)

How to: The pulsed-wave Doppler sample volume is positioned just before the pulmonary valve in the parasternal short-axis view with a zoom of RV outflow tract. A low RVOT acceleration time indicates raised pulmonary pressures.

Tips: Pay attention to the presence of a systolic notch on the RVOT spectral Doppler tracing, as it has been shown to correlate with raised pulmonary vascular resistance.[2]

Limitations:

- In patients with atrial fibrillation, the mean value of 5 sequential measurements is used
- Not applicable in certain conditions e.g. pulmonary stenosis, RVOT obstruction
- It needs to be indexed to the patients' heart rate when a patient has tachy/bradycardia

2. Tricuspid Annular Plane Systolic Excursion (TAPSE)

How to: It is measured from a modified apical four chamber view with the direction of the systolic motion of the tricuspid annulus parallel to the M-mode cursor. Limit the width of sector, onto the RV free wall. Position M-mode cursor on the lateral portion of the tricuspid annulus. Sweep velocity should be ≥50 mm/s. TAPSE reflects the base to apex shortening of the RV in systole.[2]

Tips: It has shown to have good correlation with RV ejection fraction (RVEF).

Limitations:

TAPSE is load dependent. Therefore, in patients with significant tricuspid regurgitation, may get pseudo-normalized. Furthermore, TAPSE should be interpreted with caution in the initial period after cardiac surgery as it is often reduced by 30-40%.

3. RV systolic pressure (RVSP)

How to: It is measured with continuous wave Doppler of the tricuspid regurgitant jet and applying the Bernoulli equation (RVSP = 4(TR V_{MAX})^2 + RAP) where RVSP: right ventricular systolic pressure, TR V_{MAX}: max velocity of the regurgitant jet across the tricuspid valve, and RAP is the mean right atrial pressure.

Remember that RVSP is dependent of age and body surface area.[3-5]

Tips:

- Use multiple echocardiographic views to obtain the best alignment between the direction of the jet and the CW Doppler beam and avoid underestimation of the gradient between the RV and the RA
- Measure only complete CW Doppler envelopes. Use saline or blood-saline contrast agent to enhance Doppler signal and obtain an optimal CW tracing in difficult cases
- The peak RV-RA gradient is obtained at end-expiration

Limitations:

This formula assumes that the systolic pressure in the RV is equal to the systolic pressure in the pulmonary artery. Accordingly, this formula cannot be applied where there is pulmonary stenosis, and it is not valid in cases of massive or torrential tricuspid regurgitation (triangular shape of the CW Doppler tracing of the TR jet).

RVSP is only estimated by Doppler echocardiography, and, according to the most recent guidelines, the reference method to measure pulmonary artery pressure is right heart catheterisation.

4. Fractional area change (FAC)

RV end-diastolic and end-systolic areas can be measured by planimetry, and the FAC is calculated as [(end-diastolic area − end-systolic area)/ end-diastolic area] × 100.

Tips: The use of the RV focus apical view has been reported to provide more accurate and reproducible values of FAC.[2,4]

Limitations:

Limited reproducibility due to the heavily trabeculated RV walls.

3-dimensional RV assessment

Acquisition of the 3D RV pyramidal dataset can be achieved using either a single or multi-beat approach from the RV-focused apical 4-chamber view. Notably, RV volumes and ejection fractions derived from 3D datasets acquired in the apical four-chamber view strongly correlate with measurements from the RV-focused view provided that the entire RV can be captured within the 3D dataset.[6-9] Four- to six-beat acquisitions allow for higher temporal and spatial resolution enabling more optimal identification of end-diastolic and end-systolic phases for volumetric calculations.[6-9] Current 3D analysis software employs a volumetric approach to compute the total quantity of pixels within the RV endocardial surface in systole and diastole to obtain the respective volumes. This technique overcomes geometric assumptions and minimizes acquisition variability.

RV volumes and ejection fraction measured with 3D echocardiography have demonstrated good accuracy when compared to cardiac magnetic resonance imaging (CMR).[9]

Tips:

- To obtain a complete 3DE dataset, the RV focused view from the apical approach is of paramount importance
- Patients positioned in steep left lateral decubitus, and positioning the probe more lateral than the position used for the apical views of the LV help to acquire a more complete dataset of the RV
- Identify the best timepoint during the respiratory cycle when you have the best visualization of the RV endocardium
- The use of an echocardiographic bed with a cut-out area of the mattress at the level of the apical approach is of paramount importance to acquire complete 3D datasets of the RV while preserving the patient's comfort

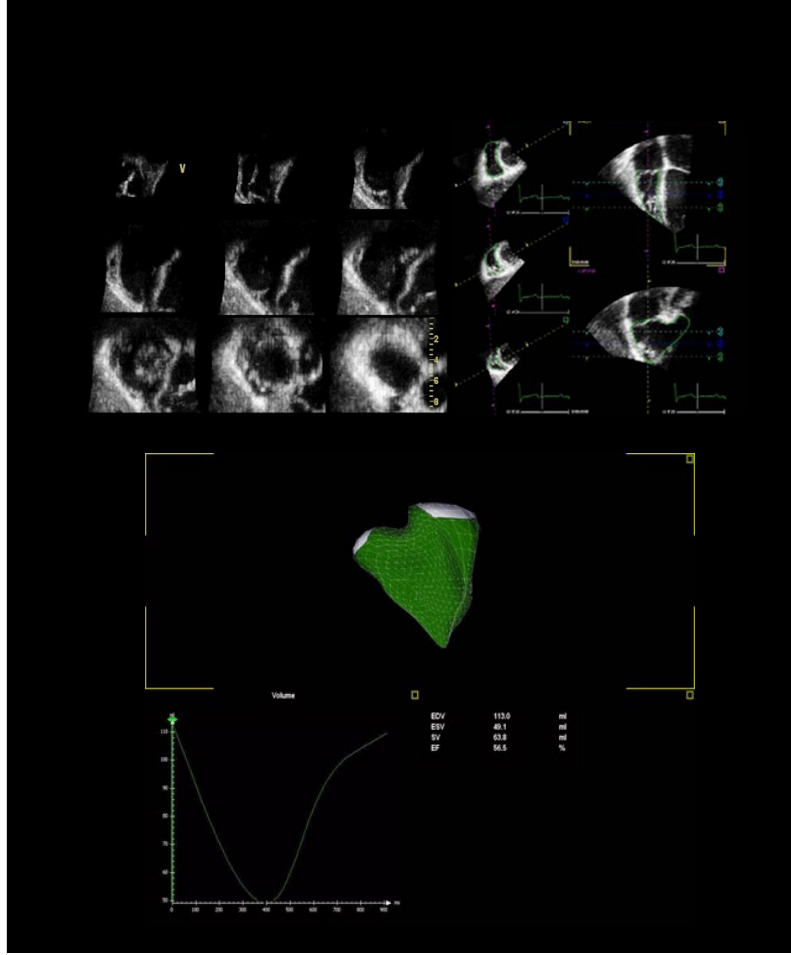

Figure 2: Three-dimensional right ventricular assessment with a vendor independent software

- Does not matter if the 2D section is foreshortened or unusual, look for the best visualisation of the endocardium and use the multi-slice display option to check that the whole RV (usually the RV anterior wall is the most difficult to include) is encompassed in the dataset
- Four- to six-beat acquisitions allow for higher temporal (minimum 20 vps) and spatial resolution enabling more optimal identification of end-diastolic and end-systolic phases for volumetric calculations
- Although the algorithm is reliable in selecting the end-diastolic and end-systolic frames, routinely check them looking at the motion of the tricuspid valve
- Trace the endocardium of compacted part of the RV wall
- Rotate the longitudinal plane to visualize the RV outflow tract and ensure that it is correctly included into the measurement
- Manual editing of the endocardial border is needed in almost every case to avoid underestimation of RV volumes
- Increase the slice thickness to improve the visualization of the endocardium
- Check the consistency of the RV and LV stroke volumes

Limitations:

- RV larger than 350 mL are difficult to be included into the 3D-echocardiography dataset (consider CMR)
- Patients with poor image quality challenge the RV chamber quantification with 3D-echocardiography (consider CMR)

RV myocardial deformation imaging

Two-dimensional strain

Similar to the left ventricle, the region of interest (ROI) of the RV is defined by the endocardial border, which is the inner contour of the myocardium, and the epicardial border, which is the outer contour of the myocardium (or in the case of the interventricular septum, the left ventricular endocardial contour of the septum).[10] Each of these contours can be either manually traced by the user or generated automatically. If they are generated automatically, the user should be allowed to check and, eventually, manually edit them. Extreme care should be taken in the definition of the ROI, since the inclusion of pericardium will result in underestimation of the measured strain. Endocardial strain measurements report the change in length of the endocardium during systole. Full wall myocardial strain refers to the average of measurements obtained over the whole myocardial thickness.[10] Measurement of RV free-wall longitudinal strain has proven prognostic value in patients with tricuspid regurgitation.[11]

Tips and tricks:

- Optimal frame rate should be 40–70 frames per second[6]
- More accurate and reproducible if data obtained from an apical RV focused view (on axis – avoid foreshortening)
- Don't extrapolate tracings if RV is dilated
- RV free wall strain is more reliable in patients with TR
- Normal values for RV free wall strain are −28.5 ± 4.8%; The normal range of RV systolic strain analysing the healthy subjects was as follows: RV global strain −24.5 ± 3.8% and RV free wall strain −28.5 ± 4.8% (lowest expected value −17 and −19%, respectively)[12]

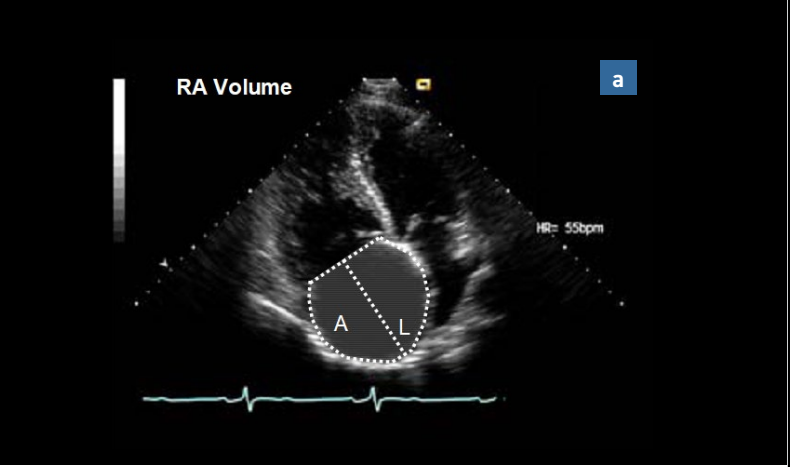

Right atrium (RA)

RA dilatation is important in the assessment of patients with TR as a part of the etiology as well as immediately related to prognostic outcomes. It is calculated in three different ways: Area-length method, summation of disk method (Simpson) or 3-dimensional imaging. Figure 3 demonstrates the various methods to assess RA size.

RA strain is calculated by the ROI placed on the RA walls in the apical four-chamber view and adjusted to RA wall thickness of approximately 2 to 3 mm, tracing from the tricuspid valve insertion to tricuspid valve insertion, which the generic software divides into six segments. To optimize tracking, manual adjustment is performed, and segments unable to track atrial wall movement are excluded from analysis. End-diastole is gated by the R wave on electrocardiography as the beginning of the cardiac cycle for RA strain. Peak longitudinal strain values from each of the six RA segments are being averaged to RA peak longitudinal strain, representing the global RA reservoir function occurring during ventricular systole.[13-15]

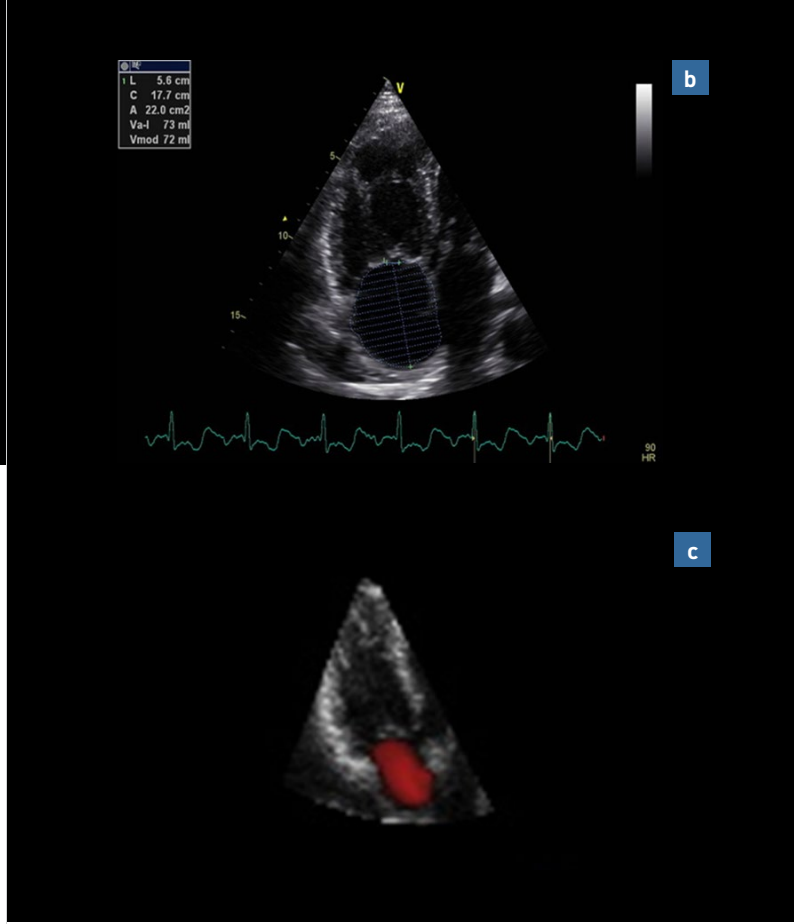

Figure 3: Right atrial assessment of size with (a) area length method (b) disk summation (c) 3-dimensional echocardiography

Transoesophageal echocardiography

Preprocedural assessment

Because of its unique geometry, multiple images of the RV are required for accurate structural and functional assessment. The most useful TEE scan planes for RV examination include the midesophageal four-chamber view, midesophageal RV inflow-outflow view, transgastric mid short-axis view, and transgastric RV inflow view.

The **midesophageal four-chamber view** is the single most useful view for assessing overall RV anatomy and global function, and allows evaluation of the apex, mid, and basal segments of RV. In the four-chamber view, the RV appears triangular compared to the elliptical LV and its length extends to only two-thirds of the length of the LV. As a result, the LV, not the RV, normally forms the cardiac apex.

The **midesophageal RV inflow-outflow view** is sometimes termed the "wrap-around view," because the right atrium (RA), RV, and pulmonary artery (PA) appear to encircle the aortic valve and left atrium, circumscribing a 180° to 270°. This view is particularly helpful for assessing motion of the RV free wall.

The **transgastric mid short-axis view** may be obtained in the horizontal scan plane with the TEE probe inserted approximately 35-40 cm from the incisors, with the tip flexed to achieve a true short-axis view. Slight clockwise (rightward) probe rotation will centre the RV in the image screen. While this view is used most often to monitor LV function, it also allows assessment of the RV free wall and ventricular septum.

Finally, the **transgastric RV inflow view** provides a long-axis view of the RV similar to the transgastric two-chamber view of the LV. To acquire this view, begin with the transgastric mid short-axis view of the RV (described on the previous page) and advance the multiplane angle to approximately 90° or until the RA and RV are seen in long-axis, with the RV inflow and tricuspid valve centered in the image. Alternatively, one develops the transgastric two-chamber view of the left atrium and ventricle and then rotates the probe clockwise (rightward) until the two right-sided chambers are displayed. Both techniques allow to obtain the same image of the RV inflow tract and the long-axis of the right atrium and ventricle.

Other TEE views may be used to supplement these four standard views in patients who have abnormal RV anatomy and function. The **midesophageal long-axis view** includes a portion of the RV outflow tract, and often the pulmonic valve can be seen anterior to the aortic valve. The **transgastric RV outflow view** provides an image with many of the same structures seen in the midesophageal RV inflow-outflow view, including the RA, RV, PA. Not only used for anatomic imaging, this view allows calculation of cardiac output from measurements of the RV outflow tract dimensions and the corresponding blood flow velocity. This view is acquired starting with the transgastric mid short-axis view, advancing the multiplane angle to approximately 110-140°, and with slight clockwise (rightward) rotation of the TEE probe. Finally, the deep transgastric RV apical view provides an image similar to the **deep transgastric long-axis view**, but focused instead on the RV, tricuspid valve, and RA. This view is acquired by slight clockwise (rightward) rotation of the probe from the deep transgastric long-axis view.

Tricuspid valve

Characteristics of different types of tricuspid regurgitation

Anatomy of the tricuspid valve

Tricuspid valve is made of four parts:

- There are usually three **leaflets** (septal, anterior and posterior), but there are many variations in healthy people
- There are usually three **papillary muscles**. The largest is the anterior papillary muscle, which gives chordae to the anterior and posterior leaflets
- The **chordal attachments**: about 17 to 36
- The **annulus**: D-shaped and nonplanar structure

Echocardiographic assessment of tricuspid valve anatomy

The accurate identification of the leaflets remains a challenge due to the considerable variability of leaflet anatomy and the multiplicity of imaging planes that can be obtained.

2D TTE standard views (*Figure 4*):

1) **Parasternal RV inflow**: The anterior leaflet (in red) is at the top of the image in ***Figure 4,*** panels d and e). Opposite may be the septal (in orange, ***Figure 4***, panel d) or posterior (in green, Figure 4, panel e) leaflet (***Figure 4***).

2) **Parasternal short-axis**: Typically, the anterior and posterior leaflets can be visualized. The anterior leaflet is on the aortic valve side. By angling the transducer towards the left ventricular outflow tract, the septal leaflet may be visualized.

3) **Apical 4-chamber**: The septal leaflet (in orange) can be clearly identified; the opposite leaflet may be the anterior leaflet (in red, ***Figure 4***, panel b) or the posterior (in green, ***Figure 4***, panel c) leaflet (***Figure 4***).

Transesophageal echocardiography – standard views

1) **4 chambers view 0°** shows the septal leaflet starting from the septum and usually the anterior leaflet facing it, at mid-esophageal level. However, it may be the posterior leaflet especially in deep esophageal views. Biplane imaging may be helpful as the anterior leaflet is seen adjacent to the aortic valve and the posterior leaflet adjacent to the posterolateral RV wall.

2) **RV inflow-outflow view at 60°** (***Figure 5, panel a***). The anterior leaflet (red color) is adjacent to the aorta and the posterior leaflet (green color) is opposite. The anterior papillary muscle can be seen at the separation between the two. If the biplane is placed between the aortic valve and the anterior papillary muscle, the septal and anterior leaflets can be seen (***Figure 5***, panel b). If the biplane is placed between the anterior papillary muscle and the RV free wall, the septal and posterior leaflets can be seen (***Figure 5***, panel c).

3) **Transgastric short-axis view** (***Figure 5, panel d***). The leaflets identification can be facilitated by the use of anatomical landmarks:[2]

   a. aortic valve (antero-septal commissure is adjacent)

   b. interventricular septum (septal leaflet is attached)

   c. anterior papillary muscle (separates the anterior leaflet from the posterior leaflet)

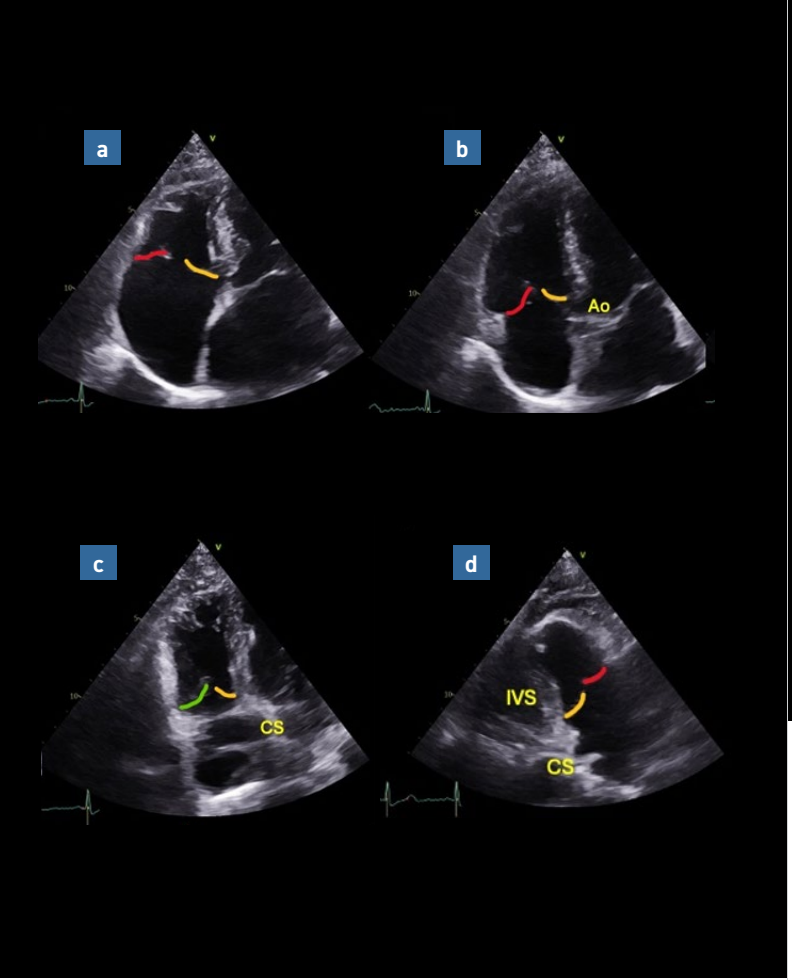

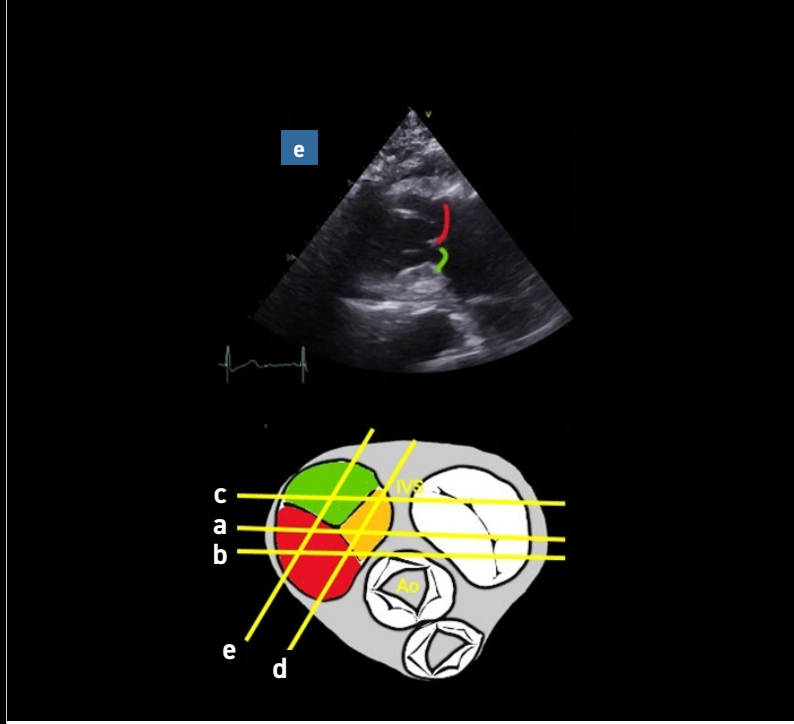

Figure 4: Tricuspid anatomy examination by TTE in an 81-year-old patient with secondary TR. The anterior leaflet is colored in red, the septal leaflet in yellow and the posterior leaflet in green. Panel F shows the different cross-section planes on an anatomical representation. Apical 4-chamber view (a, b, c). The septal leaflet is close to the IVS; In most of the cases, the opposite leaflet is the anterior (a). However, angling the transducer anteriorly (b, see the aortic valve) will image the anterior leaflet with confidence. Angling the transducer posteriorly (c, see the coronary sinus) will image the posterior leaflet. Parasternal RV inflow view (d, e): The anterior leaflet is at the top of the image. Opposite may be the septal or posterior leaflet. If the coronary sinus ostium or the interventricular septum is visible, it is most likely the septal leaflet (d). If not, it may be the posterior leaflet (e).
Abbreviations: *Ao: aortic valve, CS: coronary sinus, IVS: interventricular septum, RV: right ventricule TR: tricuspid regurgitation, TTE : transthoracic echocardiography*

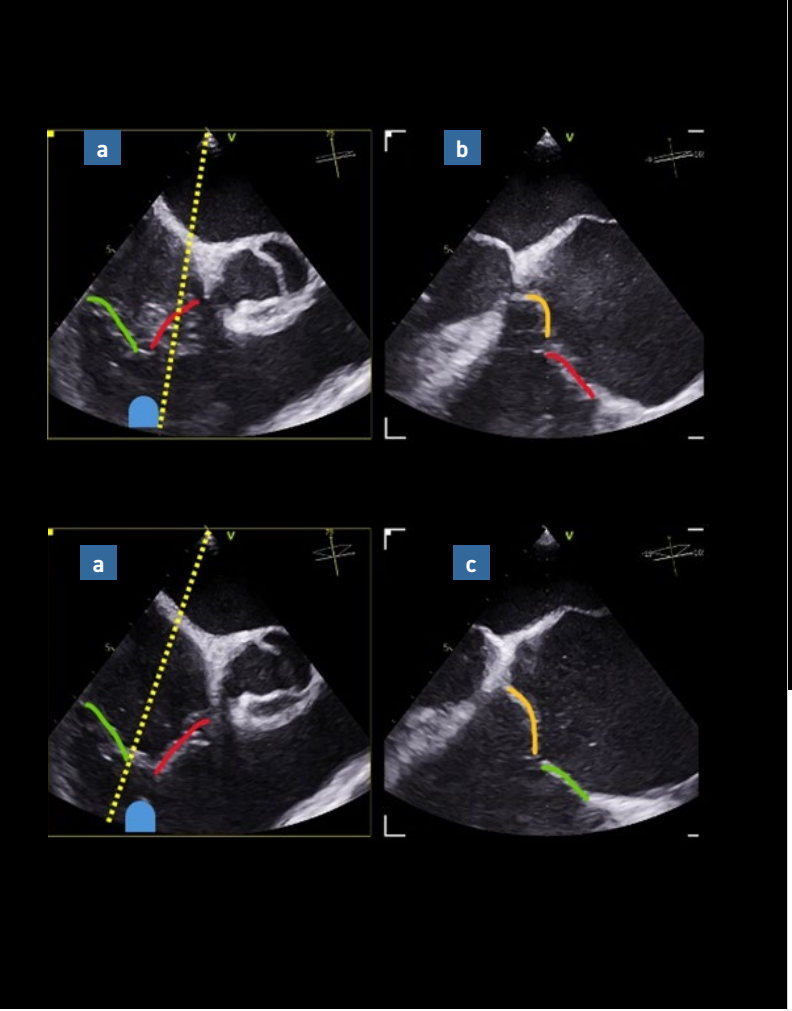

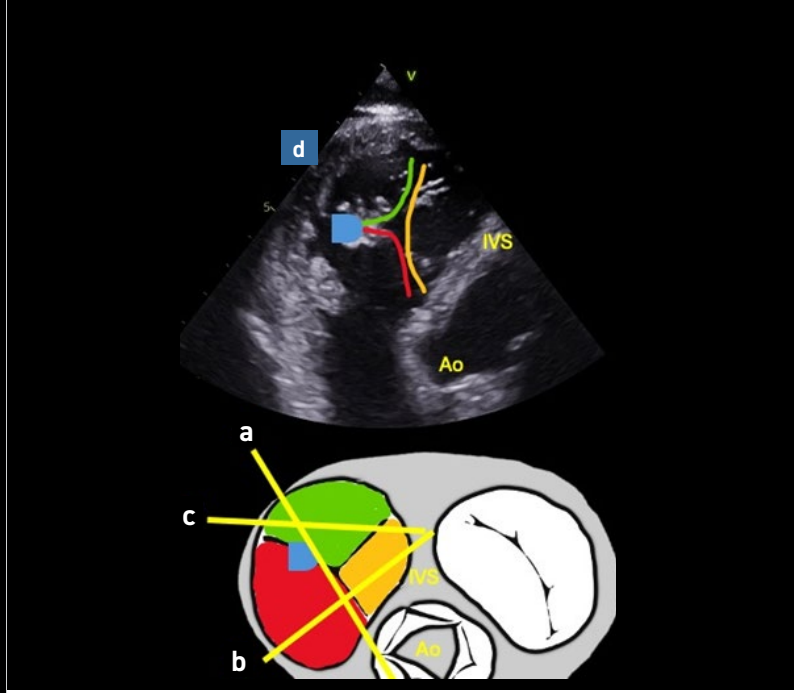

Figure 5: Tricuspid anatomy examination by TEE in an 76-year-old patient with secondary TR. The anterior leaflet is colored in red, the septal leaflet in yellow and the posterior leaflet in green. Anterior papillary muscle is in blue. Panel F shows the different cross-section planes on an anatomical representation. RV inflow-outflow view at 60° (a). The anterior leaflet is adjacent to the aorta and the posterior leaflet is opposite. The anterior papillary muscle (blue) can be seen at the separation between the two. The septal leaflet is located behind the plane of view. The use of biplane (b, c) allows it to be imaged. If the plane is placed between the aortic valve and the anterior papillary muscle, the septal and anterior leaflets can be seen (b). If the plane is placed between the anterior papillary muscle and the RV free wall, the septal and posterior leaflets can be seen (c). Transgastric short-axis view (d): Septal leaflet is adjacent to interventricular septum, aortic valve is adjacent to the anteroseptal commissure so anterior leaflet can be localized. Anterior papillary muscle (blue) is the separation between anterior and posterior leaflet.
Abbreviations: *Ao: aortic valve, IVS: interventricular septum, RV: right ventricule, TEE: transesophageal echocardiography, TR: tricuspid regurgitation*

3D echocardiography

3D tricuspid annulus imaging and analysis

Visualization of the tricuspid annulus (TA) with 3D echocardiography begins with optimization of the RV-focused apical view. Narrow-angle or full volume acquisition from this plane adequately captures the TA. Accurate measurement of TA size and function even with current multi-planar reconstruction techniques is difficult due to the nonplanarity of the annulus necessitating manual or automated initialization of the leaflet hinge points with automated interpretation throughout the cardiac cycle.[5,15]

3D TTE acquisitions of datasets including the TV can be performed from any of the conventional acoustic windows (parasternal, apical, and subcostal). There is not a specific acoustic window from which to acquire a 3D TTE dataset of the TV. The acoustic window from which the TV is best visualized by conventional 2D echocardiography is usually used to acquire a 3D dataset of the TV. However, due to the close proximity of the TV and the right ventricle to the chest wall, and the spatial orientation of the leaflets perpendicular to the direction of ultrasonography beams, an optimal 3D TTE acquisition of the TV is often best achieved from the apical approach, using an RV focused or a foreshortened 4-chamber view, which allows inclusion of the entire TV in the dataset.[15,16] Often, a parasternal long-axis view of the right chambers (with the transducer angled toward the right hip) or a parasternal short-axis view can also be used to obtain good quality 3D images of the TV. With the parasternal approach, the TV is situated in the near field, and the resulting 3D echocardiographic images may have a better spatial resolution than images acquired from the apical approach; however, because the quality of the apical window is usually better than that of the parasternal window in many adult patients, both approaches are valid as long as all 3 TV leaflets are completely visualized.[15]

Tricuspid regurgitation phenotypes

Characterizing the etiologies of tricuspid regurgitation (TR) is essential for defining patient outcomes and guiding surgical or transcatheter tricuspid valve (TV) interventions. Current state-of-the-art reviews suggest classifying TR as primary, secondary, or cardiac implantable electronic device (CIED)-related (***Table 2***).

Classification	Etiologies
Primary/Organic TR	
Degenerative	Prolapse, flail
Congenital	Ebstein anomaly, tricuspid atresia, leaflet cleft
Acquired	Infective endocarditis, rheumatic disease, carcinoid disease, traumatic, iatrogenic (biopsy, drugs, radiation therapy)
Secondary/Functional TR	
Ventricular Secondary TR	Primary pulmonary artery hypertension, Pulmonary hypertension due to left heart diseases Pulmonary hypertension due to lung diseases
Atrial Secondary TR	Atrial fibrillation, heart failure with preserved ejection fraction
CIED-related TR	
Type A (causative)	Leaflet impingement, perforation, Valvular/subvalvular adhesions/ restriction
Type B (incidental)	No tricuspid valve interference

Table 2: Classification of tricuspid regurgitation

Primary TR stems from anatomical abnormalities of the TV leaflets and/or subvalvular apparatus and is observed in only 8-10% of patients with TR (***Figure 6***). It can be caused by various conditions such as infective endocarditis, myxomatous degeneration of the TV leading to prolapse or flail TV, congenital diseases such as Ebstein anomaly, rheumatic fever, carcinoid syndrome, endomyocardial fibrosis, penetrating and non-penetrating chest trauma, and iatrogenic damage during cardiac surgery, biopsies, chest radiation therapy, or the use of medications like ergot alkaloids.

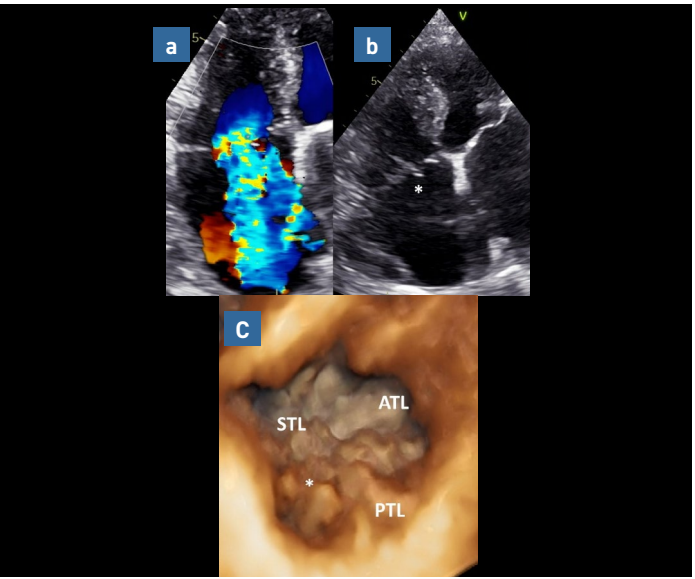

Figure 6: Patient with primary TR. An 82-year-old woman with arterial hypertension and a history of mitral valve prolapse presents with massive TR (EROA 0.61 cm²). The leaflets present excessive motion with suspected spontaneous chordae rupture(*) (panel b). Three-dimensional echocardiography confirmed extensive prolapse of the leaflets in Barlow's disease, primarily involving the septal and posterior leaflets (panel c).

Secondary TR (STR), characterized by normal leaflets in the presence of annular dilatation and/or leaflet tethering, is the most common etiology, accounting for more than 80% of TR cases. Recently, STR has been subdivided into two distinct phenotypes: **ventricular STR (V-STR)** and **atrial STR (A-STR)**[16,17] (***Figure 7***).

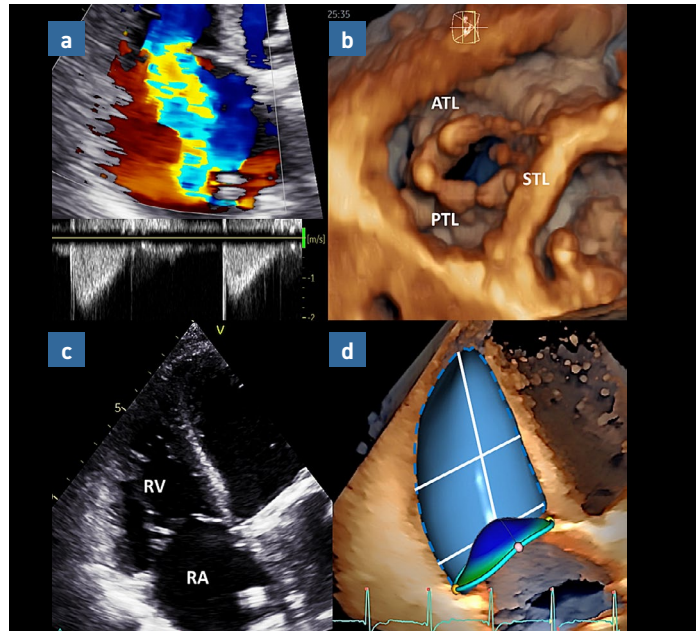

Figure 7: Patient with V-STR. A 64-year-old man with a history of post-capillary pulmonary hypertension due to previous rheumatic mitral stenosis. He presents torrential TR (EROA 0.89 cm²) (panel a). Although the leaflets appear normal, they exhibit restricted motion during systole (Carpentier IIIb) (panel b). The RV is severely enlarged (end-diastolic volume 123 mL/m², end-systolic volume 54 mL/m²), causing papillary muscle displacement and significant leaflet tethering (tenting volume 5.6 mL) (panels c and d). Additionally, both the TA and RA are dilated, with an end-systolic RA/RV volume ratio of 1.2.

- V-STR results from right ventricular (RV) dilatation and dysfunction due to pressure or volume overload, often associated with pulmonary hypertension caused by left-sided heart disease, leading to papillary muscles displacement and TV leaflet tethering. In contrast, A-STR arises from tricuspid annular (TA) and right atrial (RA) dilatation, in presence of normal RV, and occurs most commonly in patients with long-standing atrial fibrillation and/or heart failure with preserved ejection fraction. Several studies using 3D echocardiography reveal different morphological patterns of right heart remodeling in these two phenotypes. Specifically, V-STR is marked by significant TV leaflet tethering, increased tenting height, and volume in the presence of a dilated and/or dysfunctional RV with a spherical or elliptical deformation, defined by an increase in all diameter ratios and sphericity index.

- Conversely, in A-STR, TV leaflet tethering is absent or minimal, and the RV maintains normal size and function, exhibiting a remodeling pattern resembling a conical deformation shape. This is characterized by increased basal-to-mid and basal-to-longitudinal diameter ratios and a reduced sphericity index. Although both TA and RA dilation are common features of both phenotypes, the disproportionate dilatation of the RA compared to the RV, defined by an increased end-systolic RA ratio, is specific to A-STR (***Figure 8***). Specifically, an end-systolic RA area ratio ≥1.5 has been listed among the parameters supporting the diagnosis of A-STR over V-STR. However, since RA and RV enlargement are part of the right-heart remodeling process associated with severe STR, relying solely on the end-systolic RA area ratio is insufficient to distinguish between A-STR and V-STR, particularly in the later stages of the disease. Thus, some patients may exhibit features of both A-STR and V-STR, making clear categorisation difficult. Suggested anatomic and functional parameters to differentiate A-STR from V-STR, as proposed by the PCR Tricuspid Focus Group and Tricuspid Valve Academic Research Consortium (TVARC),[16] are listed in ***Table 3***.

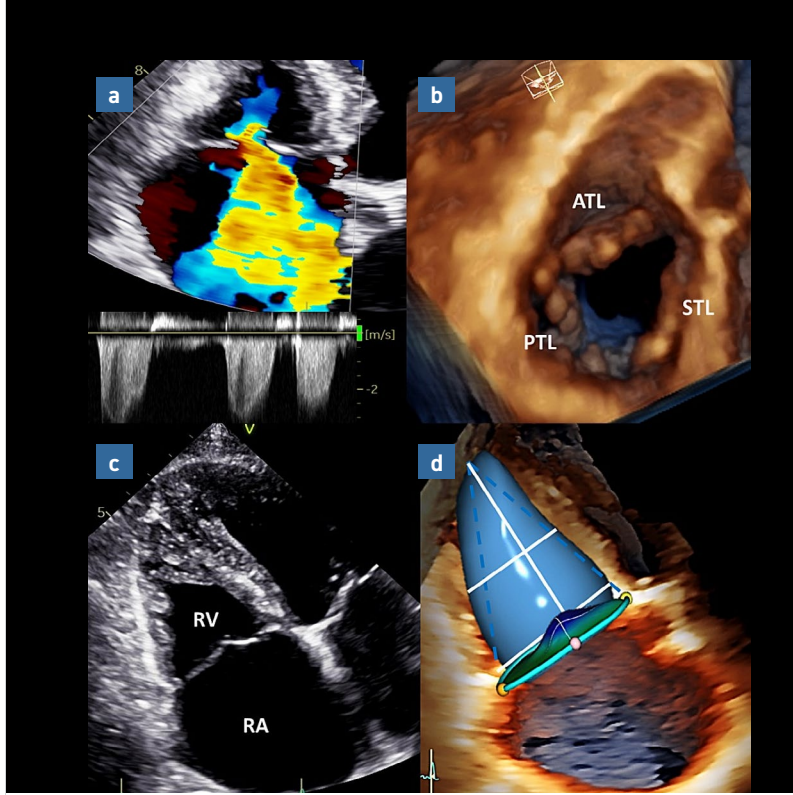

Figure 8: Patient with A-STR. A 73-year-old man with arterial hypertension and supraventricular premature contractions presents with severe TR (EROA 0.47 cm²) (panel a). The leaflets are normal with preserved systolic-diastolic motion (Carpentier Ib) (panel b). Despite a normal RV size (end-diastolic volume 77 mL/m², end-systolic volume 30 mL/m²), the RV is markedly dilated (50x43 mm) with minimal leaflet tethering (tenting volume 2.1 mL). Additionally, the RA is enlarged (98 mL/m²) with an end-systolic right atrium/right ventricular volume ratio of 1.6 (panels c and d).

	A-STR	V-STR
Leaflet morphology		
Tenting height (4Ch, mm)	≤9	>9
Tenting area (4Ch, cm^2)	<2.1	≥2.1
Tenting volume (mL)	<2.5	≥2.5
Right heart chamber size		
Mid-ventricular RVD (mm/m^2)	≤38	>38
Indexed mid-ventricular RVD (mm/m^2)	<21	≥21
RVEDV (mL/m^2)	<80	≥80
RVEDV (mL/m^2)	<21	≥21
RV sphericity index 2D	<55	≥55
RAV:RVESV ratio	≥1.5	<1.5
RV systolic function		
TAPSE (mm)	>17	≤17
FAC (%)	≥35	<35
RVFWLS (%)	≥-20	<-20
RV TDI S' (cm/s)	≥9	<9
RVEF (%)	≥50	<50
LV systolic function		
LVEF (%)	≥50	variable
Invasive pulmonary vascular hemodynamics		
PCWP (mmHg)	≤15	variable
mPAP (mmHg)	<20	usually >20
PVR (WU)	<2.0	variable

Table 3: Suggested anatomic and functional parameters to discriminate atrial secondary tricuspid regurgitation from ventricular secondary tricuspid regurgitation from the PCR Tricuspid Focus Group and Tricuspid Valve Academic Research Consortium (TVARC)

If data are discordant or incomplete (e.g. RVFWLS missing), an integrative approach based on multiple parameters is recommended.

Abbreviations: *2D: two-dimensional, 4Ch: apical four-chamber, A-STR: atrial secondary tricuspid regurgitation, CIED: cardiac implantable electronic device, EDV: end-diastolic volume, ES: end-systolic, ESV: endsystolic volume, FAC: fractional area change, LV: left ventricular, LVEF: left ventricular ejection fraction, GLS: global longitudinal strain, mPAP: mean pulmonary arterial pressure, PCWP: pulmonary capillary wedge pressure, PVR: pulmonary vascular resistance, RAV: right atrial volume, RVFWLS: right ventricular free wall longitudinal strain; RVD: right ventricular diameter, RVEF: right ventricular ejection fraction, TAPSE: tricuspid annular plane systolic excursion, TDI S: tissue Doppler systolic velocity, TR: tricuspid regurgitation, V-STR: ventricular secondary tricuspid regurgitation, WU: Woods units*

CIED-related TR (***Figure 9***) has become increasingly prevalent in recent years due to the rising number of pacemaker, implantable cardioverter defibrillator, and cardiac resynchronization therapy device implantations. CIED-related TR can be subcategorized into type A, where a causative relationship between CIED and TR is established, and type B, where no clear causative relationship is evident between CIED and TR.

The mechanisms responsible for CIED-related TR can be categorized into three groups: implantation-related, device-related, and pacing-related. Implantation-related causes are primarily associated with lead impingement, characterized by the apposition of the leaflet and lead in systole with reduced systolic leaflet excursion, lead entanglement within the subvalvular apparatus, or leaflet perforation or laceration during RV lead placement. Device-related factors include leaflet avulsion, typically occurring during lead extraction, or lead adherence to valve leaflets or subvalvular apparatus due to fibrosis and scar tissue formation. Pacing-related TR is attributed to dyssynchronous motion resulting from RV stimulation. In this context, 3D echocardiography is essential to determine the trajectory of the CIED lead and assess leaflet and lead motion.

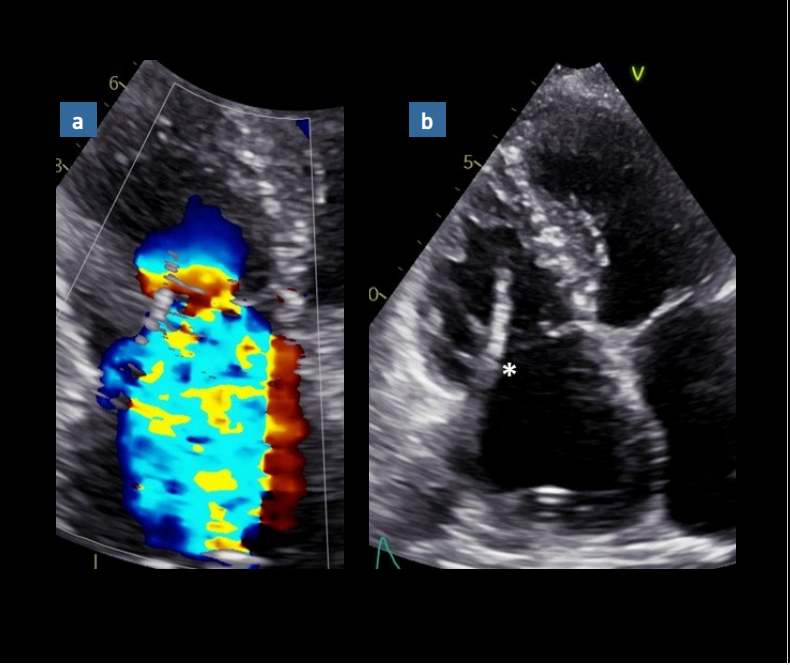

Figure 9: Patient with CIED-related TR. An 82-year-old woman with a history of permanent atrial fibrillation and dual-chamber pacemaker implantation presents with severe tricuspid regurgitation (EROA 0.58 cm²) (panel a). Echocardiography reveals the apposition of the anterior leaflet and pacemaker lead (*) during systole, reducing its excursion (panel b). This finding is confirmed by three-dimensional echocardiography from the ventricular perspective, which shows the lead impingement on the anterior leaflet, leading to a significant coaptation defect (panel c).

Another important classification of the TR mechanism is that proposed by Prof. Carpentier, which remains the most commonly used for surgical planning. Carpentier type I corresponds to normal leaflet motion, occurring in the presence of leaflet perforation (as in cases of infective endocarditis or trauma caused by catheter or lead) (Ia) or caused by TA dilatation (Ib), as seen in A-STR. Carpentier type II corresponds to excessive leaflet motion, observed in the presence of prolapse of one or more leaflets. Carpentier type III corresponds to restricted motion in diastole/systole (IIIa) as a consequence of rheumatic disease, significant calcifications, toxic valvulopathy, or in systole (IIIb), as seen in V-STR.

Quantification of tricuspid regurgitation

Quantifying tricuspid regurgitation (TR) can be difficult for several reasons: multiple regurgitation jets, changes due to respiration or loading conditions.

Characterization of the TR severity relies on an integrative assessment of multiple parameters. Current recommendations from the European Association of Cardiovascular Imaging (EACVI)[4] and the American Society of Echocardiography (ASE)[2] suggest using qualitative, semi-quantitative and quantitative parameters to quantify TR severity in 3 grades (***Table 4***). Severe TR is defined by:

- **Qualitative parameters**: a valve with a large coaptation defect (greater than 0.5 cm)/severe tenting (lack of appropriate coaptation), a continuous wave signal with a dense/often triangular with early peaking (***Figure 10***)
- **Semi-quantitative parameters**: a systolic flow reversal of the hepatic vein flow, a E wave dominant (≥1 m/s), a proximal isovelocity surface area (PISA) radius >9 mm, a vena contracta (VC) width >7 mm or a 3D VC area >75 mm^2[18]
- **Quantitative parameters**: an effective orifice area (EROA) ≥40 mm^2, a regurgitant volume (RVol) ≥45 mL or a regurgitant fraction ≥50%

Tips:

- Imagine the regurgitant jet from multiple (parasternal, apical and subcostal) views
- For the PISA method, the Nyquist limit must be >28-30 cm/sec.
- ***Figures 10*** and ***11*** describe a patient with severe tricuspid regurgitation

Tips and tricks for the TR Quantitative Echocardiographic Assessment	
TR vena contracta	Used semiquantitatively, with width >7 mm favoring severe TR and ideally performed in 2 different planes
3D TR vena contracta	Less reliable with complex orifice shapes, sensitive to color gain, and may be underestimated with multiple jets
EROA/PISA	1. Use an aliasing velocity close to 10% of peak TR velocity 2. Record multiple beats to account for TR respiratory dependency 3. Account for angle of leaflet tenting Correction for both leaflet angle and lower velocity of TR jet is essential to avoid underestimation of TR. Important limitations of EROA measurement need to be acknowledged, such as orifice shape influence on EROA reliability, uncertainty about true hemispheric shape of flow convergence, and angle correction for regurgitant flow measurement. These may yield significant underestimation of TR severity.

Table 4: Tips and tricks on tricuspid regurgitation severity assessment

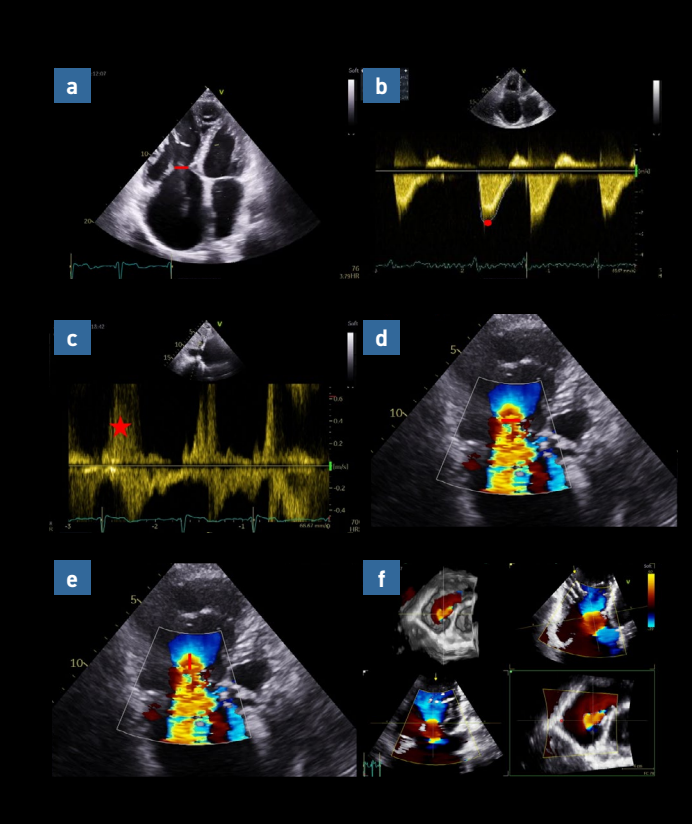

Figure 10: Example of an 84-year-old male with COPD, permanent AF for 10 years and hospitalized several times for acute heart failure. The coaptation gap was measured at 10 mm in apical 4-chamber view (red line, a), dense and triangular continuous wave signal with early peaking (red point, b), systolic flow reversal of the hepatic vein flow (red star, c), VC width at 8 mm (red line, d), PISA radius at 10 mm (red line, e) and 3D VCA at 370 mm^2. TR was considered torrential.
Abbreviations: *AF: atrial fibrillation, COPD: chronic obstructive pulmonary disease, PISA: proximal isovelocity surface area, VC: vena contracta; VCA: vena contracta area*

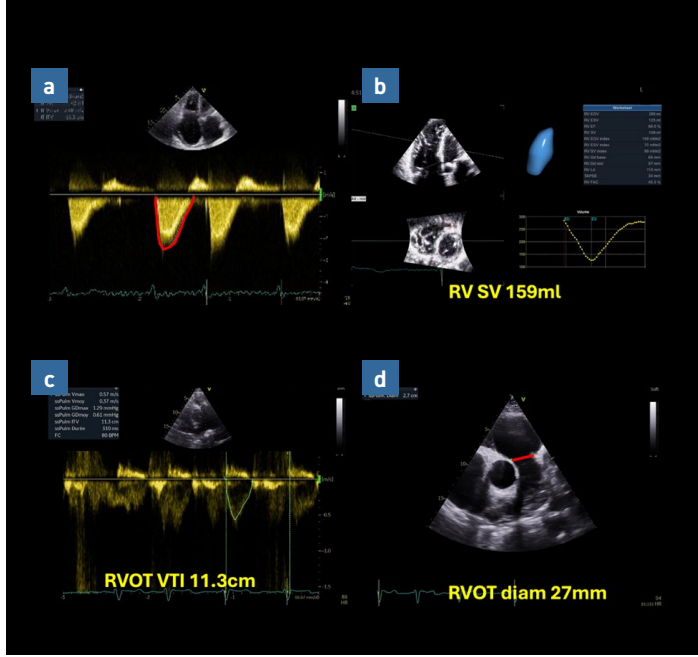

Figure 11: Same patient. The EROA was calculated at 60 mm^2 and the RVol at 90 mL using the PISA method (a). For the PISA method, the Nyquist limit must be shifted in the direction of regurgitation (here downwards) up to 40 cm/s. Using 3D, the RV stroke volume was calculated at 159 mL and using continuity equation for the RVOT, the RVOT stroke volume was calculated at 65 mL, leading to a RVol at 159-65 = 94 mL (c and d).
Abbreviations: *EROA: effective regurgitant orifice area, PISA: proximal isovelocity surface area, RV: right ventricle, RVol: regurgitant volume, RVOT: right ventricular outflow tract*

Limitations:

- The tricuspid regurgitant orifice has a complex and unpredictable shape. As a consequence, a single VC diameter can either under- or over-estimate the actual TR severity. Averaging two orthogonal diameters (i.e., apical 4-chamber and parasternal RV inflow) can improve the reliability of the measurement. The planimetry of the VC using the 3D color provides a measurement that is independent of any geometric assumption[19, 21,22]
- The PISA method is based on several geometric assumptions: the regurgitant orifice is tiny and circular, it lays on a flat plane, and the isovelocity surface is a perfect hemisphere. Unfortunately, none of them are met in patients with moderate/severe TR. The regurgitant orifice is large and of unpredictable shape (never circular); in most of patients (V.STR), there is a significant tethering of the leaflets. In these patients, correcting for the leaflet tethering angle and the low regurgitant velocity has reduced the underestimation of TR severity and has been associated with better outcome prediction[19,22]

More recently, a 5 grades classification scheme has been proposed by Hahn et Zamorano defining massive TR (VC: 14-20 mm, EROA: 60-79 mm^2, 3D VCA 95-114 mm^2) and torrential TR (VC: ≥21 mm, EROA ≥ 80 mm^2, 3D VCA ≥115 mm^2).[26] This classification has been shown to improve risk stratification of TR patients before and after transcatheter tricuspid valve intervention.

Note that all quantification parameters must be obtained from patients in euvolemic state and averaged over 3 cardiac cycles (5 in case of atrial fibrillation).

Quantification using cardiac MRI has been also proposed with a threshold regurgitant fraction >50% to define severe TR, but MRI assessment of TR is less established compared with other regurgitant lesions.

Intraprocedural assessment of tricuspid valve

Important limitations in the intraprocedural assessment of tricuspid valve are:

1. Anterior position of the tricuspid valve
2. Far field imaging
3. Poor lateral resolution
4. Acoustic shadowing from foreign material such as a pacemaker lead or prosthetic valves on the left side, significant mitral/aortic calcification or lipomatous interatrial septum

Consideration of cross-sectional imaging:

If extracardiac vascular structure assessment is required, such as the vena cava, consider multimodality imaging, as TEE can be limiting. Complementary imaging that may address tricuspid TEE limitations include **intracardiac echocardiography (ICE)** and cardiac computed tomography (CT). While the scope of this booklet is not to explain ICE technology and utility in full length, we will summarise the use of 3D ICE in tricuspid procedures.

Intraprocedural tricuspid assessment

Before the intervention starts, the preparation of the probe is of pivotal value. We ensure sterilisation of the probe and that its functioning well by testing the large and small wheels. Ensure you turn the large wheel clockwise (anteflexion) and counterclockwise (retroflexion). The small wheel controls lateral flexion: clockwise rotation flexes the probe leftward and counterclockwise flexes the probe rightward. Subsequently the anaesthetist may help the insertion of the probe and until the interventionalist is ready to start the procedure, the role of the imager is to do a comprehensive preprocedural TEE.

Tips:

- A comprehensive preprocedural TEE assessment means that you will assess all anatomical structures and ensure there are no new abnormalities/findings
- If you have difficulty in visualising the tricuspid valve or it is foreshortened, then a pillow under patients right shoulder may help co-axiality

Four-chamber view

- Typically obtained at a transducer angle of 0° to 25°
- Both leaflets should be visualized throughout the cardiac cycle because this view is occasionally used intraprocedurally to assess clip grasping
- Adjustments to the right-left flexion wheel can help optimize the images
- Leaflet length and assessment of any tethering or prolapse can also be evaluated
- If present, the RV pacemaker wire should be carefully examined as it crosses the valve to evaluate for any leaflet impingement

Assessment of tricuspid regurgitation:

Colour-flow image of TR can then be obtained to measure vena contracta and, with baseline shift, proximal isovelocity surface area (PISA) diameter.

Continuous-wave Doppler should be obtained through the TR jet to capture systolic and diastolic flow.

If massive/torrential TR then RVSP is not feasible through the Bernoulli equation as it will be underestimated.

RV inflow/outflow and commissural view

- Typically obtained between 60° and 90°
- Tricuspid leaflets are better seen from commissural view with the septal-anterior commissure toward the right side of the valve (closer to the aortic valve) and the posterior-septal commissure toward the left side (further away from the aortic valve)
- Angle should be adjusted to show the widest extent of TR coming through the valve, and the location of the regurgitation (ie, anterior, posterior, both) should be demonstrated
- PISA, vena contracta, and continuous-wave Doppler should be captured

Tip: This view is analogous to the commissural view for transcatheter mitral valve repair. Instead of localizing the medial-to-lateral location and width of the regurgitation between the anterior and posterior leaflets of the mitral valve, the anterior-to-posterior location and width of the regurgitation are demonstrated with respect to the septal-anterior and septal-posterior commissures. Similar to the mitral commissural view, an X-plane cursor can be directed through the valve to show the orthogonal image to the right. If the cursor is directed through the tricuspid valve closer to the aortic valve, the orthogonal view will show the septal and anterior leaflets—a potential grasping view at that location.

Important views intraprocedurally

- ✓ The clip can be advanced where the cursor is directed.
- ✓ Clip arms should be visualized when open in the orthogonal view.
- ✓ Similarly, if the cursor is directed toward the left (further from the aortic valve), the orthogonal view will show the septal and posterior leaflets at that location. Multiple image clips should be obtained with and without colour as the cursor is swept across the tricuspid valve.
- ✓ It is important to see the tricuspid leaflets throughout the cardiac cycle, especially in the regions where TR is located because these will be potential grasping views during the procedure.

Long-axis view—intent-to-clip view

- Long-axis view is obtained at 140° to 180° and is similar to the orthogonal view obtained from the commissural view
- This view is frequently used for grasping during the procedure (and thus is often referred to as the intent-to-clip view)
- Visualization of both of the leaflets throughout the cardiac cycle is important
- Leaflet length and assessment of any tethering or prolapse can also be evaluated
- As with the other views, PISA, vena contracta, and continuous-wave Doppler should be captured

3-dimensional images

- For three-dimensional imaging, the highest frame rates should be obtained, with and without colour. When you obtain the 3D, ensure you select multiple cycles in order to achieve the highest possible frame rate, with or without colour
- Even in atrial fibrillation, the systolic time interval remains relatively constant, and with retrospective capture, images can be selected with minimal stitch artefacts with multiple-beat capture
- Images can be obtained from any view which offers visualisation of all three leaflets, but the commissural view is often useful to ensure that part of the aortic valve is included in the image for orientation purposes

Multiplanar Reconstruction (MPR)

In the planning of any TV-TEER procedures, the aetiology for TR needs to be assessed in depth. This is often done in a separate study prior to the intervention. As recommended by the American Society of Echocardiography in its published standards for TEE in structural heart diseases interventions, 5 measurements before TV-TEER can be performed using 3D MPR. Often, echocardiographers use a mid-oesophageal view at 60°-to-80° to visualize the septal leaflet as their primary structure of interest. The clip is then advanced toward the TV using a bicaval view, with frequent use of orthogonal planes for correct localization and to avoid inadvertent injury to the interatrial septum or other cardiac structures. With the TEER device in the right atrium, a switch to 60°-to-80° view is then preferred to span the septal leaflet and the commissures. The trajectory of the device to its target zone should then be assessed with initial rotational adjustments. To evaluate the rotation of the clip, a short-axis view of the TV is necessary, which is often best seen in a transgastric view. Here, localization of gaps and colour Doppler assessment are integral in determining the ideal target site and orientation of the clip. Multiplane imaging is used frequently at this step, as well as when the deployment system is advanced in the ventricle, to help refine positioning. Grasping the leaflets and securing the clip are performed in mid- and/or deep-oesophageal view, which is often perceived as one of the challenging steps during the procedure. After confirmation of adequate grasp and reduction in TR (best assessed by vena contracta area), the clip can be released.

Multiplanar reconstruction relates to the fact that frequent probe manipulation can be avoided (also to the advantage of reduced risk for oesophageal injury), and in situations of acoustic shadowing from an aortic prosthesis, an alternative acoustic window can be used, and 3D live MPR is used to re-create desired 2D views.

Deep oesophageal window

- Instrumental view when there is shadowing of the tricuspid leaflets (particularly the septal leaflet) on mid-oesophageal views
- Images should be obtained from the deep oesophageal position just above the gastroesophageal junction
- From this position, the atrial septum and septal mitral annulus are taken out of the field of view, and the leaflets are often better visualized
- Four-chamber, RV inflow-outflow/commissural, long-axis, and 3D views can be repeated from this window if needed

Transgastric images

- Essential for screening as well as intraprocedural use
- The probe is advanced into the stomach and flexed to obtain a short-axis view of the mid-LV. It is then withdrawn until the tricuspid valve leaflets are visible
- Angle is rotated anywhere between 0° and 60° to view all three commissures
- Adjustments to right-left flexion can help optimize the view. Finally, probe flexion can be adjusted to focus on the leaflet tips, where the gaps between leaflets appear the smallest
- Properly identifying the gap width is essential because this variable is a key determinant of eligibility for TTVR and procedural success
- From this view, the location of TR along the commissures can be assessed, and the gap widths at those locations can be determined
- Instrumental for procedural planning (clip location, size, and number of clips)
- If an RV pacing lead is present, this view helps localize where the lead crosses the valve with respect to the commissures, whether there is excessive lead motion, and whether the lead is located close to the potential grasping locations
- Anatomic tricuspid variants can occasionally be identified on 3D imaging but are generally easier to identify from the transgastric short-axis images given the higher spatial resolution

Tip: Transgastric view is critical for TEER device arm alignment and positioning, as well as for the assessment of leaflet insertion. Be careful to avoid multiple manipulations from that view as there is a risk of oesophageal tear.

Measurement of cardiac output pre and post device implantation:

- Assessing the cardiac output before and after implantation is an important step towards the understanding of an objective clinical improvement
- Furthermore, a useful comparison is to obtain the RVOT VTI prior to intervention and after, from the deep transgastric view – when the procedure is successful, an increase of VTI after the implantation is expected to be seen

On ***Figures 12-14***, we describe 3 different patient cases on intraprocedural echocardiographic.

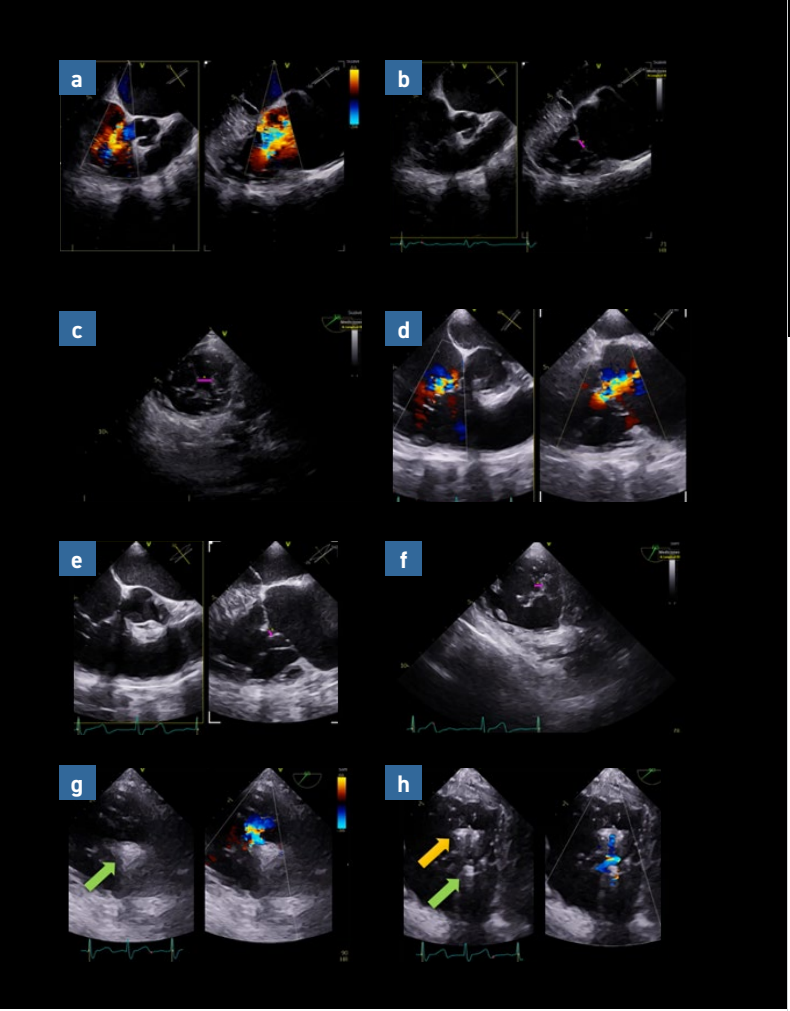

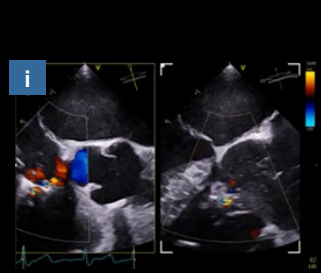

Figure 12: **Case 1: Optimization before treatment –** A 85-year-old woman with hypertension, dyslipidaemia and long-standing atrial fibrillation was referred from another centre for T-TEER evaluation. The patient was symptomatic with asthenia, dyspnoea NYHA functional class II-III, abdominal distension, and anorexia. The treatment included high doses of diuretics (160 mg furosemide, 25 mg hydrochlorothiazide, 50 mg eplerenone). In the blood work, there was an increase of alkaline phosphatase and gamma glutamyl transaminase. Right heart catheterization showed PAP 31/12 mmHg, PCP 21 mmh and V wave of 19 mmHg. The TOE showed a 4-leaflet tricuspid valve (type IIIB) with massive TR with biplane vena contracta of 14.5 mm and a gap of 11 mm [panels a-c]. Because of the presence of a big gap for T-TEER patient was admitted 48h before the intervention to intensify diuretic treatment. The screening with TOE during the intervention showed a reduction of the gap (5 mm) and vena contracta (9 mm) having now a favourable anatomy for T-TEER [panels d-f]. A Triclip XTW was implanted in antero-septal position [panel g], and additional Triclip XTW was implanted between P1 and de septal leaflet [panel h] with a good result: mild TR [panel i], mean gradient of 0.7 mmHg and no complications. Patient was discharged 24h after the intervention maintaining previous diuretic treatment. At 6 month follow-up, patient had NYHA FC I-II, no oedemas, no abdominal distension and normal appetite. The echocardiography showed as sustained good result with mild to moderate residual TR.

(a-c) baseline transoesophageal echocardiogram: biplane from inflow-outflow view with colour (a) and without colour (b) with gap measurement [pink line]; (c) transgastric short axis view with gap measurement. (d-e) TOE after intensive diuretic treatment: biplane from inflow-outflow view with colour (d) and without (e) , transgastric short axis view (f)]. (g-i) TOE during T-TEER: transgastric short axis view with colour compare after first Triclip implantation [green arrow] (g) and after second Triclip implantation [yellow arrow] (h): biplane from inflow-outflow view with colour showing the final result.

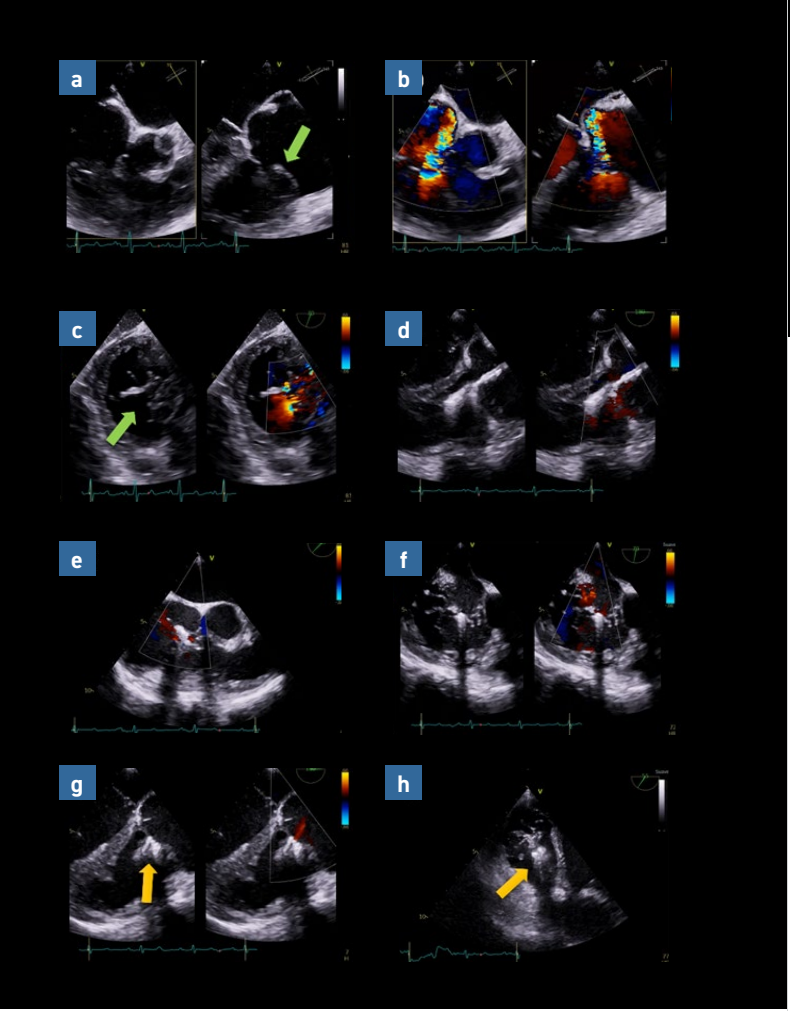

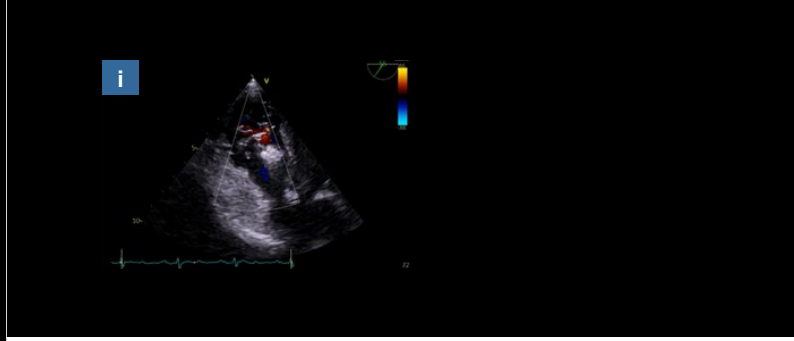

Figure 13: **Case 2: Degenerative TR –** Forty-nine-year-old man with well controlled HIV treated with antiretrovirals, hepatic cirrhosis Child B secondary to hepatitis C. Patient complained with progressive dyspnoea, now with short exertion dyspnoea but no oedemas. An echocardiogram was performed showing severe TR, the right ventricle had a moderate enlargement with a mil dysfunction at that moment. The TOE showed a severe degenerative TR with prolapse of the anterior leaflet [panels a-c]. The aetiology of the prolapse was considered due to previous right heart catheterizations, but the exact moment of the occurrence was not clear. Last right heart catheterization showed a pulmonary pressure of 47/21/31 mmHg, PCP 7 mmHg. The patient was presented in the valve team, the surgery was ruled out due to cirrhosis and T-TEER was proposed. A Triclip XT was implanted in anteroseptal position with mild residual TR and no significant gradient [panels d-i]. Patients was hospital discharged 24h after intervention with no complications. The 12-month follow-up showed as sustained good result with mild residual TR, patient was in function class I-II NYHA.

(a-c) baseline transoesophageal echocardiogram: biplane from inflow-outflow view (a) [green arrow points the prolapse of the anterior leaflet] and with colour (b); transgastric short axis view colour compare (c). (d-i) TOE during Triclip implantation, before Triclip release [(d) long axis view colour compare, (e) inflow-outflow view with colour, (f) deep inflow-outflow view colour compare] and final result [(g) long axis view colour compare, transgastric short axis view without (h) and with colour(i)] [yellow arrow points the Triclip].

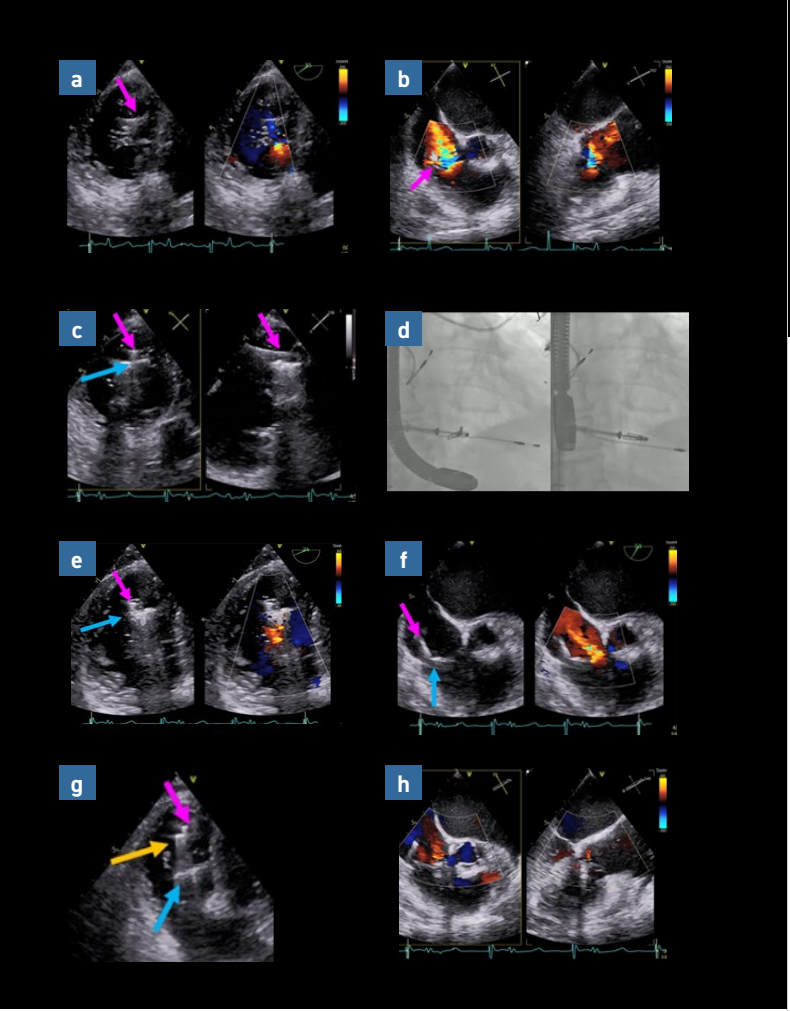

Figure 14: **Case 3: pacemaker lead –** 83-year-old female with hypertension, chronic atrial fibrillation with pacemaker implantation 7 years ago. Patient complained with dyspnoea NYHA functional class II-III, ankle oedema and abdominal perimeter increase. The TOE showed a massive TR, the aetiology was mainly functional (chronic atrial fibrillation) despite a mild interaction of the pacemaker lead with the posterior part of the septal leaflet. The right heart catheterization showed a pulmonary artery pressure of 41/4/12 mmHg with PCP of 16 mmHg. It was decided to perform a T-TEER. A first Triclip XT was implanted in postero-septal position isolating the pacemaker lead in the commissure; a second Triclip XT was implanted in antero-septal position treating the functional TR. The result was mild TR and no significant gradient. The patient was discharged 24 hours after the intervention with no complication. The one-year follow-up showed a mild TR and mean gradient of 3 mmHg, patient was in function class I-II and no congestive signs. Baseline transoesophageal echocardiogram: (a) transgastric short axis view colour compare [pink arrow points the pacemaker lead], (b) inflow-outflow view with biplane colour. First Triclip XT implantation [blue arrow] trying to isolate pacemaker lead in the postero-septal commissure: (c) transgastric short axis view with bi-plane, (d) fluoroscopic view before and after grasping. Result after first Triclip deployment showing the remaining TR: (e) transgastric short axis view colour compare, (f) inflow-outflow view colour compare. Second Triclip implantation [yellow arrow]: (g) positioning of the clip in antero-septal position in a transgastric short axis view, (h) final result after second Triclip deployment showing mild TR in a inflow-outflow view with biplane and colour, (i) final fluoroscopic view.

Transcatheter tricuspid valve replacement (TTVR) system

EVOQUE valve

- Technical considerations relate to mechanism of anchoring (leaflets vs. annulus vs. chords), annulus shape/size, delivery approach and IVC course to the annulus
- IVC approach and angulation relative to the tricuspid annulus can influence device delivery, limit coaxiality and impact procedural success
- Different TTVR systems have different anchoring mechanisms and thus different imaging requirements. In general, these intraprocedural imaging requirement are less for TTVR than for leaflet approximation or annular devices
- After positioning of a pre-shaped guidewire carefully toward the RV apex and in a central position across the TV, the delivery system is advanced to the RA where it is flexed across the TV
- After advancement of the delivery capsule below the valve, position and trajectory are optimised and anchors are exposed below the leaflets but above the papillary muscle heads
- As the valve is exposed and expands, the anchor tips become positioned subannular to capture the leaflets
- When there is adequate leaflet capture and positioning below the annulus, the valve is fully deployed and released, with careful system removal without interaction with the valve

Tip: The EVOQUE system (Edwards Lifesciences) is a 28Fr transfemoral venous system which can allow for a 44 mm, 48 mm or 52 mm diameter valve implant. The delivery system is capable of primary and secondary flexion as well as adjustable depth. The valve is made of bovine pericardium, is trileaflet, has a nitinol frame with nine anchors and a fabric skirt.

LuX-Valve:

- There are 3 critical steps during device implantation, which reply on intraprocedural imaging guidance
- Step 1: As a first step, after advancing the distal end of the delivery system into the right ventricle (RV), the delivery system must be sufficiently deep, and in the centre of and perpendicular to the TV annulus. The depth and co-axiality of the delivery system relative to the TV annulus is standard assessed on TEE using mid- and deep-oesophageal RV inflow–outflow X-plane views. The tip of the delivery system should be positioned ~4 cm distal to the TV annulus
- LuX-Valve depends on native leaflet grasping and not radial forces (lateral movement)
- Final and crucial step is the anchoring into the IVS (septal)
- Important to verify the correct position of the clips on imaging before further deployment
- Mid-oesophageal RV inflow-outflow and transgastric X-plane views are used to confirm that both leaflet grasping clips are below the TV leaflets. Typically, the clips (also called 'rabbit ears') grasp the anterior leaflet (lateral side) and over-ride the anterior papillary muscle that is located at the commissure between anterior and posterior leaflets

- After expansion of the LuX-Valve, it is important to assure contact of the septal tongue with the IVS, and this throughout the entire cardiac cycle. The angle of insertion of the delivery system already results in the septal tongue being deployed facing towards the IVS
- Co-axiality of the septal tongue relative to the IVS is assessed on TEE using a deep transgastric view
- The correct anterior-posterior and co-axial position relative to the septum is acquired by flexing/unflexing the delivery system using the flex wheel and rotating the device's inner core using the rotation knob, respectively, guided by transgastric TEE
- Before pushing the anchor out of the needle holder, it is of critical importance to verify that there is good apposition of the septal tongue with the IVS—and this throughout the entire cardiac cycle. In some cases, this may be challenging relying on TEE imaging

Tip: The LuX-Valve (Jenscare Biotechnology, Ningbo, China) is a 32Fr flexible delivery system with a bovine pericardial valve on a nitinol valve stent that has an atrial disc, an interventricular septal anchor "tongue" and two expanded polytetrafluoroethylene-covered graspers. It has four valve sizes (30 to 55 mm) and eight disc sizes to treat annular diameters of 25 to 50 mm. It is delivered via mini right thoracotomy or transatrial approach and is radial force-independent unlike other TTVR devices. This is designed to minimise force-related complications of conduction disturbance and RCA impingement but may be at a trade-off for increased risk of paravalvular regurgitation.

Heterotopic caval valve implantation

- SVC valve has a central belly to better prevent dislodgement, a long skirt to reduce paravalvular leak and an uncovered superior segment to allow innominate vein flow
- SVC stenting is performed with a stiff wire from the right femoral vein to either the right subclavian or internal jugular vein
- Valve deployment should start high so that there can be some gentle downward device traction to improve stability and is recapturable to 80% deployed
- For IVC deployment, the IVC stent has a short-covered section and its superior aspect should be near the RA junction. The valve is deployed again starting superior with downward traction to land between the RA and the hepatic vein
- Imaging considerations to ensure anatomic suitability include sequential anteroposterior measurements of the SVC (maximum 34 mm) and IVC (maximum 43 mm), length of SVC to middle of perpendicular right PA and SVC-to-RA length and length of IVC from RA junction to hepatic veins (at least 10 mm)
- SVC stenting can be done in patients with CIED with leads trapped behind the stent
- This device avoids TV/RV anatomical exclusions and can be fluoroscopically-guided avoiding general anaesthesia

Direct annuloplasty

The Cardioband adjustable annuloplasty system[31,32] includes the implant and three main accessories: (a) The implant is a polyester sleeve with radiopaque markers spaced 8 mm apart (b) TF Delivery system: The Cardioband delivery system consists of the implant delivery system and the 25F transseptal steerable sheath. (c) Implantable metal anchors and anchor delivery shafts: Implantable stainless steel, 6 mm long anchors, is used to fasten the Cardioband implant to the annulus. Between 12 and 17 anchors are implanted using a delivery shaft. The anchors are fully repositionable and retrievable until deployed. (d) Size adjustment tool: This tool is connected over the implant wire and is used to control the implant adjustment spool and the implant size.

Tips and tricks (***Figure 15***):

- Guide the delivery system into the right atrium
- The delivery system is steered, until the tip of the system is placed over the anteroseptal commissure
- Verify the first anchoring location with TEE
- The anchor should be placed close to the leaflet hinge, as anterior as possible in the annulus, close to the anteroseptal commissure
- Following confirmation of the location with 3D TEE, coronary angiography is performed to rule out the risk of damage of the right coronary artery
- The first anchor is delivered and implanted using the anchor delivery drive inside the catheter through the Cardioband implant fabric and into the annulus tissue
- The anchor is released after proper anchoring is checked with push-and-pull testing under echocardiographic and standardized fluoroscopic guidance
- The Cardioband implant is deployed until the radiopaque marker of the catheter channel reaches the next marker on the implant. The catheter tip is then navigated, by actuating the steering knobs, to the next anchoring point using echocardiographic guidance. These actions are repeated until the implant catheter tip reaches the last anchoring site on the posterior commissure
- The last anchor is then deployed and the implant disconnected from the system is subsequently removed
- The band is then cinched to reduce the tricuspid annulus size gradually while assessing the reduction of the tricuspid regurgitation

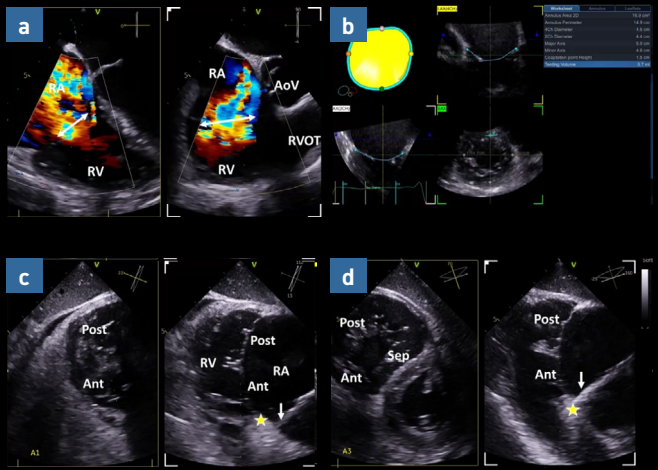

Figure 15: **Direct annuloplasty with the Cardioband system (Edwards Lifesciences, CA) –** Panel a shows the biplanar midesophageal views with 4-chamber view as reference plane and the short-axis view as the perpendicular one. The vena contracta of the regurgitant jet is measured (13x16 mm). Using specific software, the area, perimeter and maximum and minimum diameters of the tricuspid valve annulus can be measured (16.9cm^2; 14.9 cm, 5.0 cm and 4.6 cm, respectively) (panel b). The first anchor is the crucial starting point of the procedure to ensure good tissue anchoring and without damaging the right coronary artery (panel c). From the transgastric view taking as reference plane the short-axis where the anteroseptal commissure can be defined the perpendicular view allows the definition of the hinge point (star) and the visualization of the first anchor (arrow). Subsequently, the following anchors are placed always checking proper angle of anchoring at the level of the hinge point, on adequate tissue and without damaging the right coronary artery on fluoroscopy (panel d). At the level of the posterior annulus, multiplanar reformation planes aligned through the catheter and the hinge point level allows guidance of the procedure (panel e) and once the band is deployed, the cinching process starts progressively (panel f, arrows indicating the position of the band) reducing the severity of the regurgitant jet (panel g, reduction of the vena contracta to 4x5 mm) and the size of the tricuspid annulus (panel h: area, perimeter and maximum and minimum diameters of the tricuspid valve annulus 9.2 cm^2; 11 cm, 3.8 cm and 3.0 cm, respectively).

2D and 3D intracardiac echocardiography

Intracardiac echocardiography (ICE) has the ability to overcome many of the acoustic shadowing issues as well as thoracic and oesophageal pathology that can limit traditional TEE imaging. 3D ICE has been used in the field of transcatheter tricuspid annuloplasty procedures and is recently becoming recognized as an adjunctive imaging strategy with 2D ICE catheters for tricuspid transcatheter edge to edge repair (TEER) procedures. With improving ICE catheter technology, the application of 3D imaging with multiplanar reconstruction (MPR)-guided leaflet grasp and confirmation in tricuspid TEER procedures has added value beyond the use of more traditional 2D ICE. As application of advanced 3D ICE technologies emerges, it is essential to understand the fundamentals and advanced teamwork of this technology to drive appropriate tricuspid TEER outcomes.[27,28]

Post procedural assessment[30] Figure 16

- Residual tricuspid regurgitation post tricuspid interventions may be very complex to be assessed
- VC width which may be difficult to assess of multiple orifices are present (preferably by averaging measurements obtained from two orthogonal views) and PISA radius remain useful measures to assess TR severity after TTVI
- One of the most reliable parameters for assessing TR after TTVI is considered 3D VCA planimetry, which is less affected by the different TTVI devices used
- Using quantitative parameters derived from the flow convergence method (EROA and RegVol) can be used in TR grading after TTVI, especially in patients who have undergone T-TEER, annuloplasty, or orthotopic valve implantation. When multiple regurgitant orifices areas, PISA cannot be measured
- The calculation of RegFr may also be affected by TTVI, as the diastolic flow restriction caused by the TTVI device may lead to an overestimation of diastolic SV. However, it is still possible to calculate RegFr after TTVI if total RV SV is measured using other methods, such as 3DE or CMR, and RegVol is quantified by PISA. Alternatively, in patients with isolated TR, Reg Vol can be measured as the difference between left and right SV measured by 3DE or CMR
- RVOT velocity time integral from the TOE views before and after the procedure may be useful to assess success of the intervention
- Multiplanar reconstruction is very useful to assess the orientation and severity of regurgitant jets around the device

Figure 16: Overview of the strengths and limitations of the various echocardiographic parameters used to assess (residual) TR severity or paravalvular leak after TTVI and divided per type of TTVI

Parameter	T-TEER	TV annuloplasty	TTVR
Qualitative parameters			
Jet area	• Remains dependent on colour gain settings and the driving pressures • Preferably used to define the origin of the jet (e.g., multiple jets after T-TEER) and jet direction • No validation yet of jet area quantification	• Remains dependent on colour gain settings and the driving pressures • Preferably used to define the origin of the jet and jet direction	• Remains dependent on colour gain settings and the driving pressures • Normally no residual valvular TR, yet mainly used to detect (the origin of) paravalvular leakage
Density and shape of the TR CW Doppler spectrum	Analogous to preprocedural evaluation • T-TEER devices can potentially create TS, which should be checked before clip-release and during follow-up	Analogous to preprocedural evaluation	Analogous to preprocedural evaluation • Postprocedural inflow gradient dependent on loading conditions, yet longitudinal follow-up may be used to evaluate prosthetic valve thrombosis
Hepatic vein flow reversal	Analogous to preprocedural evaluation • Depends on RA compliance, which may be altered after TTVI • May not be reliable in patients with atrial fibrillation (de novo induced after TTVI) and paced rhythm with retrograde atrial conduction	Analogous to preprocedural evaluation • Depends on RA compliance, which may be altered after TTVI • May not be reliable in patients with atrial fibrillation (de novo induced after TTVI) and paced rhythm with retrograde atrial conduction	Analogous to preprocedural evaluation • Depends on RA compliance, which may be altered after TTVI • May not be reliable in patients with atrial fibrillation (de novo induced after TTVI) and paced rhythm with retrograde atrial conduction
RA/RV and annular remodeling	• Leaflet approximation may cause reduction in TV annular size • TV annular size reduction is best assessed in biplane mode (noncircular annulus) • Mandatory evaluation after TTVI to evaluate reduction in RA and RV size as well as longitudinal and radial function (longitudinal function may be more altered after T-TEER compared with radial function; importance of longitudinal follow-up) • Acute postprocedural decrease in RV FAC, (partly) recovering during follow-up • Clips may cause acoustic shadowing/artifacts complicating adequate RA endocardial delineation • Measures of RV-PA coupling could be useful, taking into account the change in loading conditions after TTVI	• TV annuloplasty causes significant reduction in TV annular size • TV annular size reduction best assessed in biplane mode (noncircular annulus) • Mandatory evaluation after TTVI to evaluate reduction in RA and RV size as well as longitudinal and radial function (longitudinal function may be more altered after TV annuloplasty compared with radial function; importance of longitudinal follow-up) • Acute postprocedural decrease in RV FAC, (partly) recovering during follow-up • Annuloplasty band causes acoustic shadowing/artifacts complicating adequate RA and/or RV endocardial delineation • Measures of RV-PA coupling could be useful, taking into account the change in loading conditions after TTVI	• Acute postprocedural decrease in RV FAC, (partly) recovering during follow-up • Significant acoustic showing/artifacts due to the prosthesis complicating adequate RA and/or RV endocardial delineation

Figure 16: Overview of the strengths and limitations of the various echocardiographic parameters used to assess (residual) TR severity or paravalvular leak after TTVI and divided per type of TTVI

Parameter	T-TEER	TV annuloplasty	TTVR
Semi-quantitative parameters			
VC	• Remains partially dependent on flow rate and the driving pressure • Preferably the average of two orthogonal views should be used: cave acoustic shadowing/ artifacts • The use of the biggest VC measure has been proposed; adding multiple measures of VC width from multiple jets is not yet validated	Analogous to preprocedural evaluation	If residual TR is present, then analogous to preprocedural evaluation
VCA (3D)	• Remains dependent on color gain settings and the spatial resolution of 3D echocardiographic color • Multiple jets can be measured and summed	Analogous to preprocedural evaluation	If residual TR is present, then analogous to preprocedural evaluation
PISA	• Device will mechanically interfere with the shape of the proximal flow, deviating it even more from the hypothetical hemispheric shape, resulting in an overestimation of the TR severity	Analogous to preprocedural evaluation • Annuloplasty band may cause acoustic shadowing/ artifacts complicating adequate PISA evaluation	• Most trustworthy parameter after TTVI and least influenced by the various TTVI devices • Difficult to use intraprocedurally
Doppler volumetric method	• Can be applied in multiple or eccentric jets • Diastolic flow restriction caused by the TTVI device results in diastolic SV overestimation • Can be used when RV SV is measured by 3D echocardiographic volumetric methods or CMR measurements • Difficult to use intraprocedurally	• Annuloplasty band causes acoustic shadowing/artifacts complicating adequate TV annular sizing • Diastolic flow restriction caused by the TTVI device results in diastolic SV overestimation • Can be used when RV SV is measured by 3D echocardiographic volumetric methods or CMR measurements • Difficult to use intraprocedurally	• TV prosthesis may cause acoustic shadowing/ artifacts complicating adequate TV annular sizing • Difficult to use intraprocedurally
3D echocardiographic volumetric method	• Most trustworthy parameter after TTVI and least influenced by the various TTVI devices • Can be applied in multiple or eccentric jets • Difficult to use intraprocedurally	• Most trustworthy parameter after TTVI and least influenced by the various TTVI device • Difficult to use intra-procedure	• Most trustworthy parameter after TTVI and least influenced by the various TTVI devices • Difficult to use intraprocedurally

Abbreviations: *CW: Continuous-wave, TS: tricuspid stenosis, TTVR: transcatheter TV replacement*

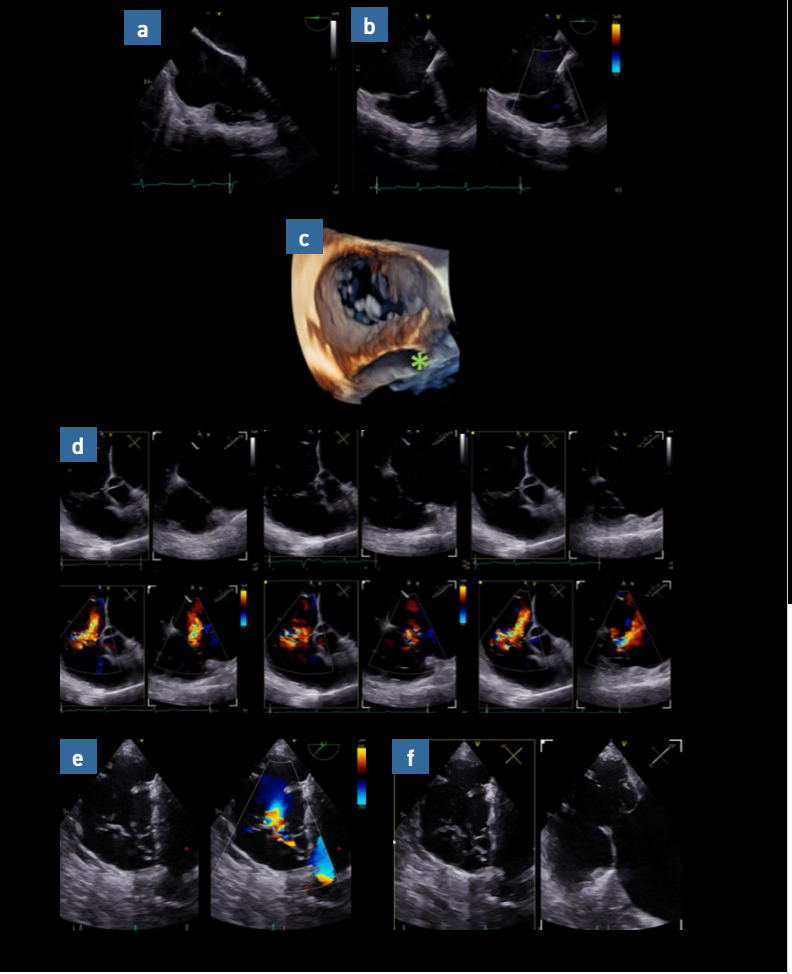

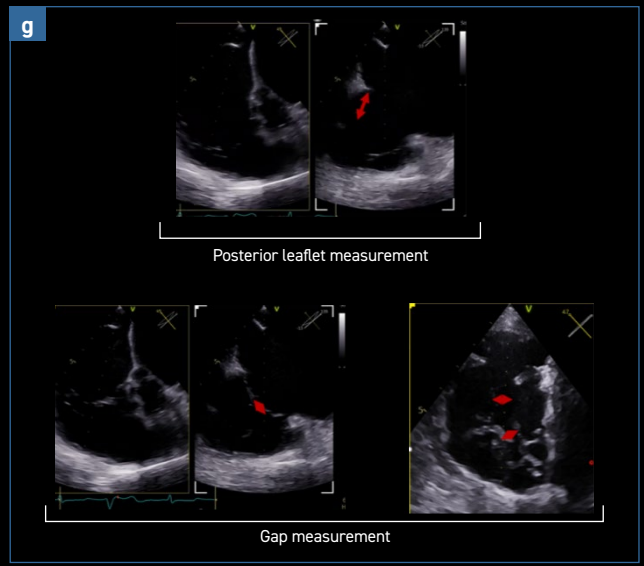

Figure 17: Main planes for tricuspid valve screening: a) 4 chamber view focused on the tricuspid valve at 0° mid-esophageal plane; b) 4 chamber view focused on the tricuspid valve at 0° deep-esophageal plane; c) 3D view of the tricuspid valve from the right atrium, asterisk marks the position of the aortic valve; d) inflow-outflow view of the right ventricle at 35-70° with biplane showing the long axis of the valve, a valve sweep is performed from the antero-septal zone towards the posterior-septal area with and without color; e) short axis view of the tricuspid valve at transgastric plane 40-60° with color compare; f) short axis view of the tricuspid valve at transgastric plane 40-60° with biplane; g) main measurements of the tricuspid valve performed during tricuspid regurgitation screening.

The report based on the TOE screening of tricuspid valve should include the following: quality of the visualization of the valve at mid-esophageal and transgastric levels, morphology of the tricuspid valve (number of leaflets and commissures), anatomy of the septal leaflet (length and restriction if present), gap (measured at the tip of the leaflets in the transgastric short axis view and/or at the inflow-outflow view with biplane).

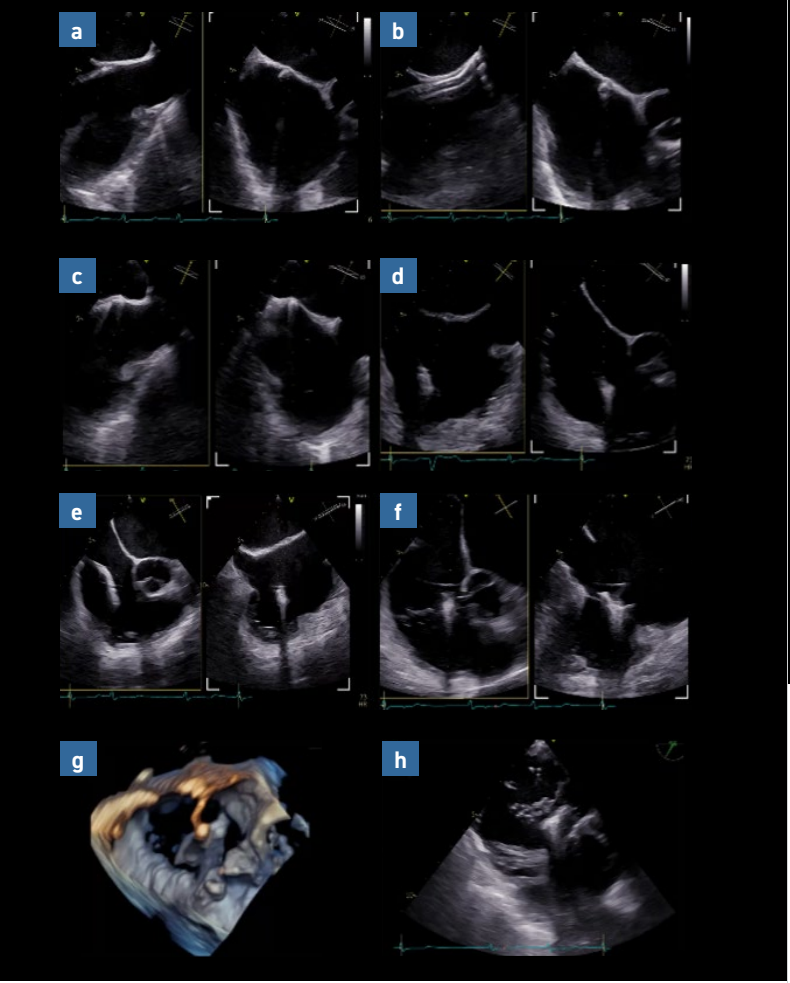

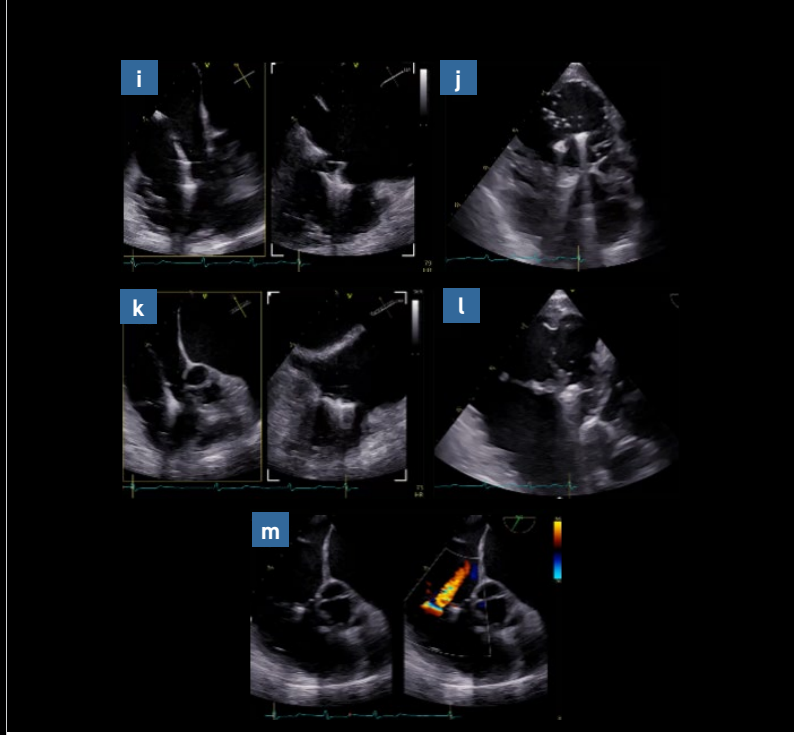

Figure 18: Echo guidance of a percutaneous tricuspid valve repair with Triclip system. a) to d) bi-cava view with inverted biplane: a) wire in superior vena cava, b) guiding catheter in superior vena cava, c) Triclip towards interatrial septum after its exposure in right atrium, d) Triclip flexing towards the tricuspid valve; e) and f) inflow-outflow view with biplane with the trajectory of the Triclip in the right atrium with Triclip closed (e) and opened (f); g) Triclip orientation evaluation with 3D and h) transgastric short axis view before crossing the valve; i) inflow-outflow view with biplane after entering in the right ventricle; j) Triclip orientation evaluation with transgastric short axis view after approaching the leaflets from the right ventricle; k) inflow-outflow view with biplane for grasping; l) leaflet insertion evaluation in transgastric short axis view; m) color evaluation after first Triclip implantation at mid-esophageal level with color compare.

In case more clips are needed c) to m) steps will be repeated after to ensure there is no significant gradient across the valve.

References:

1. Ho SY, Nihoyannopoulos P. Anatomy, echocardiography, and normal right ventricular dimensions. Heart 2006 Apr;92 Suppl 1(Suppl 1):i2-13. doi: 10.1136/hrt.2005.077875.
2. Lang RM, Badano LP, Mor-Avi V, Afilalo J, Armstrong A, Ernande L, Flachskampf FA, Foster E, Goldstein SA, Kuznetsova T, Lancellotti P, Muraru D, Picard MH, Rietzschel ER, Rudski L, Spencer KT, Tsang W, Voigt JU. Recommendations for cardiac chamber quantification by echocardiography in adults: an update from the American Society of Echocardiography and the European Association of Cardiovascular Imaging. Eur Heart J Cardiovasc Imaging 2015 Mar;16(3):233-70. doi: 10.1093/ehjci/jev014.
3. Armstrong DW, Tsimiklis G, Matangi MF. Factors influencing the echocardiographic estimate of right ventricular systolic pressure in normal patients and clinically relevant ranges according to age. Can J Cardiol 2010 Feb;26(2): e35-9. doi: 10.1016/s0828-282x(10)70004-0.
4. Galderisi M, Cosyns B, Edvardsen T, Cardim N, Delgado V, Di Salvo G, Donal E, Sade LE, Ernande L, Garbi M, Grapsa J, Hagendorff A, Kamp O, Magne J, Santoro C, Stefanidis A, Lancellotti P, Popescu B, Habib G; 2016–2018 EACVI Scientific Documents Committee; 2016–2018 EACVI Scientific Documents Committee. Standardization of adult transthoracic echocardiography reporting in agreement with recent chamber quantification, diastolic function, and heart valve disease recommendations: an expert consensus document of the European Association of Cardiovascular Imaging. Eur Heart J Cardiovasc Imaging 2017 Dec 1;18(12):1301-1310. doi: 10.1093/ehjci/jex244.
5. Augustine DX, Coates-Bradshaw LD, Willis J, Harkness A, Ring L, Grapsa J, Coghlan G, Kaye N, Oxborough D, Robinson S, Sandoval J, Rana BS, Siva A, Nihoyannopoulos P, Howard LS, Fox K, Bhattacharyya S, Sharma V, Steeds RP, Mathew T. Echocardiographic assessment of pulmonary hypertension: a guideline protocol from the British Society of Echocardiography. Echo Res Pract 2018 Sep;5(3):G11-G24. doi: 10.1530/ERP-17-0071.
6. Randazzo M, Maffessanti F, Kotta A, Grapsa J, Lang RM, Addetia K. Added value of 3D echocardiography in the diagnosis and prognostication of patients with right ventricular dysfunction. Front Cardiovasc Med 2023 Dec 21:10:1263864. doi: 10.3389/fcvm.2023.1263864. eCollection 2023.
7. Ahmad A, Li H, Wan X, Zhong Y, Zhang Y, Liu J, Gao Y, Qian M, Lin Y, Yi L, Zhang L, Li Y, Xie M. Feasibility and Accuracy of a Fully Automated Right Ventricular Quantification Software With Three-Dimensional Echocardiography: Comparison With Cardiac Magnetic Resonance. Front Cardiovasc Med 2021 Oct 21:8:732893. doi: 10.3389/fcvm.2021.732893. eCollection 2021.
8. Partington SL, Kilner PJ. How to Image the Dilated Right Ventricle. Circ Cardiovasc Imaging. 2017 May;10(5):e004688. doi: 10.1161/CIRCIMAGING.116.004688. PMID: 28495824.
9. Grapsa J, O'Regan DP, Pavlopoulos H, Durighel G, Dawson D, Nihoyannopoulos P. Right ventricular remodelling in pulmonary arterial hypertension with three-dimensional echocardiography: comparison with cardiac magnetic resonance imaging. Eur J Echocardiogr. 2010 Jan;11(1):64-73. doi: 10.1093/ejechocard/jep169. Epub 2009 Nov 24. PMID: 19939819.
10. Badano LP, Kolias TJ, Muraru D, Abraham TP, Aurigemma G, Edvardsen T, D'Hooge J, Donal E, Fraser AG, Marwick T, Mertens L, Popescu BA, Sengupta PP, Lancellotti P, Thomas JD, Voigt JU; Industry representatives; Reviewers: This document was reviewed by members of the 2016–2018 EACVI Scientific Documents Committee. Standardization of left atrial, right ventricular, and right atrial deformation imaging using two-dimensional speckle tracking echocardiography: a consensus document of the EACVI/ASE/Industry Task Force to standardize deformation imaging. Eur Heart J Cardiovasc Imaging 2018 Jun 1;19(6):591-600. doi: 10.1093/ehjci/jey042.
11. Smith BC, Dobson G, Dawson D, Charalampopoulos A, Grapsa J, Nihoyannopoulos P. Three-dimensional speckle tracking of the right ventricle: toward optimal quantification of right ventricular dysfunction in pulmonary hypertension. J Am Coll Cardiol. 2014 Jul 8;64(1):41-51. doi: 10.1016/j.jacc.2014.01.084. PMID: 24998127.
12. Morris DA, Krisper M, Nakatani S, Köhncke C, Otsuji Y, Belyavskiy E, Radha Krishnan AK, Kropf M, Osmanoglou E, Boldt LH, Blaschke F, Edelmann F, Haverkamp W, Tschöpe C, Pieske-Kraigher E, Pieske B, Takeuchi M. Normal range and usefulness of right ventricular systolic strain to detect subtle right ventricular systolic abnormalities in patients with heart failure: a multicentre study. Eur Heart J Cardiovasc Imaging 2017 Feb;18(2):212-223. doi: 10.1093/ehjci/jew011. Epub 2016 Feb 11.
13. Gavazzoni M, Badano LP, Pugliesi GM, Penso M, Hădăreanu DR, Ciampi P, Fisicaro S, Oliverio G, Heilbron F, Tomaselli M, Muraru D. Assessing Right Atrial Size in Patients with Tricuspid Regurgitation: Importance of the Right Ventricular-Focused View. Eur Heart J Cardiovasc Imaging 2024 Jul 25:jeae186. doi: 10.1093/ehjci/jeae186.
14. Tomaselli M, Radu DN, Badano LP, Perelli FP, Heilbron F, Cascella A, Gavazzoni M, Hădăreanu DR, Mihaila S, Oliverio G, Penso M, Caravita S, Baratto C, Fisicaro S, Parati G, Muraru D. Right Atrial Remodeling and Outcome in Patients with Secondary Tricuspid Regurgitation. J Am Soc Echocardiogr 2024 May;37(5):495-505.
15. Nishihara T, Takaya Y, Nakayama R, Yoshida Y, Toh N, Miyoshi T, Nakamura K, Yuasa S. Prognostic value of right atrial function in patients with significant tricuspid regurgitation. ESC Heart Fail 2024 Aug 2. doi: 10.1002/ehf2.14846. Online ahead of print.
16. Muraru D, Hahn RT, Soliman OI, Faletra FF, Basso C, Badano LP. 3-Dimensional Echocardiography in Imaging the Tricuspid Valve. JACC Cardiovasc Imaging. 2019 Mar;12(3):500-515. doi: 10.1016/j.jcmg.2018.10.035. PMID: 30846124.

17. Hahn RT, Lawlor MK, Davidson CJ, Badhwar V, Sannino A, Spitzer E, Lurz P, Lindman BR, Topilsky Y, Baron SJ, Chadderdon S, Khalique OK, Tang GHL, Taramasso M, Grayburn PA, Badano L, Leipsic J, Lindenfeld J, Windecker S, Vemulapalli S, Redfors B, Alu MC, Cohen DJ, Rodés-Cabau J, Ailawadi G, Mack M, Ben-Yehuda O, Leon MB, Hausleiter J; TVARC Steering Committee. Tricuspid Valve Academic Research Consortium Definitions for Tricuspid Regurgitation and Trial Endpoints. J Am Coll Cardiol. 2023 Oct 24;82(17):1711-1735.

18. Muraru D, Badano LP, Hahn RT, Lang RM, Delgado V, Wunderlich NC, Donal E, Taramasso M, Duncan A, Lurz P, De Potter T, Zamorano Gómez JL, Bax JJ, von Bardeleben RS, Enriquez-Sarano M, Maisano F, Praz F, Sitges M. Atrial secondary tricuspid regurgitation: pathophysiology, definition, diagnosis, and treatment. Eur Heart J. 2024 Mar 14;45(11):895-911.

19. Tomaselli M, Penso M, Badano LP, et al Clinical Impact of Correcting the PISA Method to Quantitate Secondary Tricuspid Regurgitation. J Am Soc Echocardiograph 2024 (in press).

20. Andreas M, Burri H, Praz F, Soliman O, Badano L, Barreiro M, Cavalcante JL, de Potter T, Doenst T, Friedrichs K, Hausleiter J, Karam N, Kodali S, Latib A, Marijon E, Mittal S, Nickenig G, Rinaldi A, Rudzinski PN, Russo M, Starck C, von Bardeleben RS, Wunderlich N, Zamorano JL, Hahn RT, Maisano F, Leclercq C. Tricuspid valve disease and cardiac implantable electronic devices. Eur Heart J. 2024 Feb 1;45(5):346-365.

21. Dahou A, Levin D, Reisman M, Hahn RT. Anatomy and Physiology of the Tricuspid Valve. JACC Cardiovasc Imaging. 2019 Mar 1;12(3):458–68.

22. Hahn RT, Weckbach LT, Noack T, Hamid N, Kitamura M, Bae R, et al. Proposal for a Standard Echocardiographic Tricuspid Valve Nomenclature. JACC Cardiovasc Imaging. 2021 Jul 1;14(7):1299–305.

23. Grapsa J, Praz F, Sorajja P, Cavalcante JL, Sitges M, Taramasso M, Piazza N, Messika-Zeitoun D, Michelena HI, Hamid N, Dreyfus J, Benfari G, Argulian E, Chieffo A, Tchetche D, Rudski L, Bax JJ, Stephan von Bardeleben R, Patterson T, Redwood S, Bapat VN, Nickenig G, Lurz P, Hausleiter J, Kodali S, Hahn RT, Maisano F, Enriquez-Sarano M. Tricuspid Regurgitation: From Imaging to Clinical Trials to Resolving the Unmet Need for Treatment. JACC Cardiovasc Imaging 2024 Jan;17(1):79-95. doi: 10.1016/j.jcmg.2023.08.013. Epub 2023 Sep 20.

24. Hahn RT. State-of-the-Art Review of Echocardiographic Imaging in the Evaluation and Treatment of Functional Tricuspid Regurgitation. Circ Cardiovasc Imaging. 2016;9(12).

25. Lancellotti P, Moura L, Pierard LA, Agricola E, Popescu BA, Tribouilloy C, et al. European Association of Echocardiography recommendations for the assessment of valvular regurgitation. Part 2: mitral and tricuspid regurgitation (native valve disease). Eur J Echocardiogr J Work Group Echocardiogr Eur Soc Cardiol. 2010 May;11(4):307–32.

26. Zoghbi WA, Adams D, Bonow RO, Enriquez-Sarano M, Foster E, Grayburn PA, et al. Recommendations for Noninvasive Evaluation of Native Valvular Regurgitation: A Report from the American Society of Echocardiography Developed in Collaboration with the Society for Cardiovascular Magnetic Resonance. J Am Soc Echocardiogr Off Publ Am Soc Echocardiogr. 2017 Apr;30(4):303–71.

27. Hahn RT, Zamorano JL. The need for a new tricuspid regurgitation grading scheme. Eur Heart J Cardiovasc Imaging. 2017 Dec 1;18(12):1342–3.

28. Hamid N, Aman E, Bae R, Scherer M, Smith TWR, Schwartz J, Rinaldi M, Singh G, Sorajja P. 3D Navigation and Intraprocedural Intracardiac Echocardiography Imaging for Tricuspid Transcatheter Edge-to-Edge Repair. JACC Cardiovasc Imaging 2024 Apr;17(4):441-447. doi: 10.1016/j.jcmg.2024.02.005.

29. Chadderdon SM, Eleid MF, Thaden JJ, Makkar R, Nakamura M, Babaliaros V, Greenbaum A, Gleason P, Kodali S, Hahn RT, Koulogiannis KP, Marcoff L, Grayburn P, Smith RL, Song HK, Lim DS, Gray WA, Hawthorne K, Deuschl F, Narang A, Davidson C, Zahr FE. Three-Dimensional Intracardiac Echocardiography for Tricuspid Transcatheter Edge-to-Edge Repair. Struct Heart 2022 Aug 10;6(4):100071. doi: 10.1016/j.shj.2022.100071. eCollection 2022 Aug.

30. Badano LP, Tomaselli M, Muraru D, Galloo X, Li CHP, Ajmone Marsan N. Advances in the Assessment of Patients With Tricuspid Regurgitation: A State-of-the-Art Review on the Echocardiographic Evaluation Before and After Tricuspid Valve Interventions. J Am Soc Echocardiogr 2024 Jul 17:S0894-7317(24)00356-0. doi: 10.1016/j.echo.2024.07.008.

31. Nickenig G, Weber M, Schüler R, Hausleiter J, Nabauer M, von Bardeleben RS, Sotiriou E, Schäfer U, Deuschl F, Alessandrini H, Kreidel F, Juliard JM, Brochet E, Latib A, Montorfano M, Agricola E, Baldus S, Friedrichs KP, Deo SH, Gilmore SY, Feldman T, Hahn RT, Maisano F. Tricuspid valve repair with the Cardioband system: two-year outcomes of the multicentre, prospective TRI-REPAIR study. EuroIntervention 2021 Feb 5;16(15):e1264-e1271. doi: 10.4244/EIJ-D-20-01107.

32. Davidson CJ, Lim DS, Smith RL, Kodali SK, Kipperman RM, Eleid MF, Reisman M, Whisenant B, Puthumana J, Abramson S, Fowler D, Grayburn P, Hahn RT, Koulogiannis K, Pislaru SV, Zwink T, Minder M, Dahou A, Deo SH, Vandrangi P, Deuschl F, Feldman TE, Gray WA; Cardioband TR EFS Investigators. Early Feasibility Study of Cardioband Tricuspid System for Functional Tricuspid Regurgitation: 30-Day Outcomes. JACC Cardiovasc Interv 2021 Jan 11;14(1):41-50. doi: 10.1016/j.jcin.2020.10.017.

PCR

TRICUSPID

Focus Group